T.C.

ALTINBAS UNIVERSITY

Institute of Graduate Studies

Information Technologies

# USING DEEP LEARNING AND MEDICAL DATA CLASSIFICATION FOR PREDICTING BACTERIAL SKIN INFECTION

Sura Abdulameer Nayyef AL-DABBAGH

Master of Science

Supervisor

Asst. Prof. Dr. Abdullahi Abdu IBRAHIM

Istanbul, 2021

# USING DEEP LEARNING AND MEDICAL DATA CLASSIFICATION FOR PREDICTING BACTERIAL SKIN INFECTION

by

**Sura Abdulameer Nayyef AL-DABBAGH**

Information Technologies

Submitted to the Institute of Graduate Studies

in partial fulfillment of the requirements for the degree of

Master of Science

ALTINBAŞ UNIVERSITY

2021

The thesis titled "USING DEEP LEARNING AND MEDICAL DATA CLASSIFICATION FOR PREDICTING BACTERIAL SKIN INFECTION" prepared and presented by Sura Abdulameer Nayyef AL-DABBAGH was accepted as a Master of Science Thesis in Information Technologies.

___________________________________
Asst. Prof. Dr. Abdullahi Abdu IBRAHIM

Supervisor

Thesis Defense Jury Members:

| | | |
|---|---|---|
| Asst. Prof. Dr. Abdullahi Abdu IBRAHIM | School of Engineering and Natural Sciences, Altinbas University | ___________________ |
| Asst. Prof. Dr. Muhammad Ilyas | School of Engineering and Natural Sciences, Altinbas University | ___________________ |
| Asst. Prof. Dr. Tareq Abed MOHAMMED | Computer Science , IMAM Jaafar AL-Sadiq University | ___________________ |

I certify that this thesis satisfies all the requirements as a thesis for the degree of Master of Science.

Approval Date of Institute of Graduate Studies: ____/____/____

All information in this document was collected and provided in compliance with academic rules and ethical behavior. I also declare that, as required by these rules and behavior, I have properly cited and referenced all non-original material and performance..

Sura Abdulameer Nayyef AL-DABBAGH

# DEDICATION

I devote and pledge this research work to my supervisor who is salient for guiding me through whole research work as well as my family for always assisting me in my hard time.

## ACKNOWLEDGEMENTS

First and foremost, I would like to thank my supervisor Asst. Prof. Dr. Abdullahi Abdu IBRAHIM for guiding and helping me along the way in writing this dissertation. Discussing my progress, problems, and ideas with my supervisor Asst. Prof. Dr. Abdullahi Abdu IBRAHIM a couple of times every week helped me tremendously in understanding the logic behind the research. It made me better realize the technical need for this research work. He helped me by looking outside of all the machine learning and network-based information, and considering the cryptocurrency-based knowledge from a more holistic perspective than just from the productivity point of view. He patiently explained to me a great number of technical details with regards to block-chain and cryptocurrency, for example how to deal with solving problems and to provide insight into the reliability of those results. Without his time and help none of this research would have been possible, and I'm grateful to him for giving me the opportunity to work on this interesting subject. I am also very thankful to my parents as well as my friends who always supported me through whole of this journey.

# ABSTRACT

## USING DEEP LEARNING AND MEDICAL DATA CLASSIFICATION FOR PREDICTING BACTERIAL SKIN INFECTION

AL-DABBAGH, Sura Abdulameer Nayyef,

M.Sc., Information Technologies, Altınbaş University,

Supervisor: Asst. Prof. Dr. Abdullahi Abdu IBRAHIM

Date: July /2021

Pages: 63

Infectious infectious diseases are one of the most common signs of disease in pharmacy. It's usually diagnosed clinically, with a clinical evaluation followed by a dermo copy images examination, a therapeutic or transdermal drug, and a histological examination.. In this study, I'll look at how deep learning techniques like CNN and health information detection can be used to forecast microbial skin disease. Big data is constantly being used to verify the effectiveness of identifying specific skin conditions. Many new methods have been developed to speed up the process while maintaining the quality of precision. In this paper, we introduced a method for predicting the likelihood of bacterial infections using machine learning and artificial neural networks, both of which are components of artificial intelligence's deep learning framework.. The data comprises nearly 3000 photographs of individuals with skin infections that are divided into two categories: malignant or benign. We used CNN and its 7 distinct frameworks to verify the relevance of photos of surface infectious diseases and conducted a comparative study to identify the best framework for this issue.. For the training, testing and validation of our dataset a well-known MATLAB R2019a software was used for this purpose. We had the great outcome using Neural Networks and Health Information Analysis, with an efficiency rate of nearly 91.303 percent in detecting skin problems..

**Keywords:** Bacterial Contaminants, Learning Techniques, Computer Vision, and Deep Neural Networks are all terms that can be used to describe infectious diseases.

# TABLE OF CONTENTS

**Pages**

# LIST OF TABLES

**Pages**

# LIST OF FIGURES

**Pages**

# LIST OF ABBREVIATIONS

| | | |
|---|---|---|
| CNN | : | Conventional Neural Network |
| DNA | : | Deoxyribonucleic Acid |
| ROS | : | Reactive Oxygen Species |
| SVM | : | Support Vector Machine |
| GPU | : | Graphic Processing Unit |

# 1. NTRODUCTION

## 1.1 INTRODUCTION

Psoriasis is an infectious fungal infection that lasts for years. Psoriasis Vulgaris has been the most widespread form of the disease, which is characterized by bright, furred inscriptions. The disorder causes skin irritation, nails, and joints on occasion [1]. It is most commonly found on the elbows, knees, and scalp. Psoriasis causes chronic itchiness due to just an elevated number of lymphocytes and blood circulation, also known as inflammation. While psoriasis induces a greater range of blood vessel produces and resulting in an imperfect stratum granulosum, increased flow of blood, and lymphocytes, the precise mechanism of rheumatoid arthritis are unclear. Psoriasis was found to be present in 1.5 to 3% of people in a Nordic study. In a 30-year obey randomized trial in Lewin conducted in 2007-2008, 11.8 percent of people aged 20 to 79 had rosacea, relative to 4.8 percent in 1979-1980 [2]. About 1970 and 2000, a set of inhabitants research revealed that the incidence of untreated rheumatoid arthritis in adults over the age of 18 had increased. It has been suggested that there is a considerable rise in the epidemic, that has been reported at least in the United States and Belgium [3]. The problem with these experiments is that they depend on personality data. A medical decision by a certified clinical doctor will be the accepted norm.. The doctor will identify particular features of the outer layer of skin during the psoriatic arthritis clinical examination: swelling, rosacea, stiffness, and intensity region. A medical indicator of Psoriasis intensity is included in the treatment process. The PASI (Psoriasis Area Severity Index) is a measure that ranks the intensity of rheumatoid arthritis on a range of 0-72. Anticipated systematic reviews, its been suggested, should look into the incidence of rheumatoid arthritis with a more systematic research design and use proven and medically confirmed psoriatic arthritis medical testing done by a doctor. Rheumatoid arthritis supporting facts obviously varies among research, but there could be stratified people aged going up around 20 and 39 and 50 and 69 years. [4]. This may be attributed to a variety of factors, including weather [5]. The disorder is influenced by the environment, with rising interest rates recorded in certain nations at high elevations. A research from Michigan found that the weather has an effect on rheumatoid arthritis, with 68 percent of cases reported and during winter seasons.. Owing to sun exposure, the impact of temperatures can be helpful for psoriasis in the summers [6]. Temporary differences are sadly not well accounted for in medical rosacea research.. Significant fluctuations should be controlled for in subsequent researcher, based on the knowledge of their significance and usefulness in risk exists outcomes of severity. In Ontario, fluorescent pharmacotherapy was approved in 1993. [7]. For mild to extreme rheumatoid arthritis, up treatment is an effective therapy. If other topical therapies, such as diclofenac sodium, calcitriol (vitamin D analogue), or cortisone, fail, this medication is a fine replacement (cortisone). Although the research have limited data and long confidence intervals, a research paper of potential impacts measured a satisfaction rating of about 70%. To relieve signs, about 25 treatments of therapy are required. Light care necessitates a huge commitment from the person, who must adhere to the clinical trial for 6 to 8 weeks, with 3 days each week. [8].

In a large study of 851 psoriasis participants who undergo pharmacotherapy, 53 percent provided less than 20 therapies, and about a quarter provided or less ten. The clinicians were all within a 20-kilometer radius of the Nebulizer treatments center. Just 47% of patients followed the recommended medication in order to achieve a 75% change or clearance. The explanations for lower adherence are largely due to budget limitations, scarce funds, and advanced age. The spread of the disease precise neurological processes remain unknown, but research into drugs and other therapeutic options contribute to a higher understanding of what it means and responses to questions about causal relationships. Other therapies, such as psychological approaches, have shown to be effective in treating fungal infections. Stress has been linked to exasperating the frequency of rheumatoid arthritis and lowering the life quality for those who suffer from it, according to studies published in the journal Dermatology.. The difference in how people react to stress was investigated in the Pennsylvania medical system with 4576 people who had a variety of illnesses, including psoriasis. The period between both the psychological cause of stress and the therapeutic shift of the disorder was recorded by the respondents [9]. Days passed between the pain and the disease worsening, according to the rheumatoid arthritis populace.

The burden of rheumatoid arthritis is divided into three categories: disease-related pain, disease-related effects on standard of living, as well as other psycho - social risk factors such as insomnia, panic, and suicidal tendencies, according to a study. Behavioral complications, they say, can raise psychological distress and therefore be a major factor in rosacea aggravation The burden of rheumatoid arthritis is divided into three categories: disease-related pain, disease-related effects on standard of living, as well as other psycho - social risk factors such as insomnia, panic, and suicidal tendencies, according to a study. Behavioral complications, they say, can raise psychological distress and therefore be a major element in rosacea aggravation.. When compared with untreated persons, individuals with ulcerative colitis have lower self - esteem, insomnia, suicidal tendencies, and a poor quality of life [10]. Responses to stress are influenced with how they view the stressful situation.. Physicians with a high level of condition anxiety are less likely to clear their skin of complications than patients with lower level of anxiety. Laser therapy strengthened inflammatory acne aspects including illness and bacterial infection discomfort, but had little impact on the emotional fellow human, according to Luck and coworkers..

## 1.2 MOTIVATION

In hospital treatment, the benefits of neural networks have been widely used. Machine learning methods for disease diagnosis, diagnosis, medication, and remedy advice have been applied in various segments of the field of medicine... It is typically diagnosed clinically, with an internal medical assessment accompanied by dermoscopy images investigation, a ct scan, and histology if necessary. CNN employs complex technologies to detect edges from a vast health boost data, which it then applies to analysis. In the last two decades, CNN's popularity has skyrocketed. . The field of CNN is increasingly expanding, as the computing capacity of computers continues to improve with each day. As a result, CNN models have greater precision and make better use of computational services. The aim of the project is to investigate a computer learning-based method that can be learned and produces comprehensive performance.; CNN Based frameworks, more precisely, to identify skin infectious diseases more effectively. As a result, we're doing a comparison of the various Neural networks that have already been established to identify intrusion and correlations in any picture.

Previous work

In this progressive world of science and technology, One of most common infections in the body is severe bacterial infection.. Detecting skin infections in different stages are fundamental and decisive. With the development of medical science and technology, researchers and scholars have already invented to detect skin cancer in various efficient techniques. To familiarize with the existing systems and works related to our purpose, we have inspected a large number of works and related papers.

[11] described a method for detecting skin problems that was well-thought-out. They suggested an image-processing-based approach for detecting cancer. The pictures they fed into their process were of skin conditions that looked as though they were infected. They before the their photos and improved the picture quality during the first stage.. They used texture features and an automated thresholding procedure to tag the photos. The exert significant of the photos were then removed, and tumor region study was applied. Exert different were chosen because they were the most important elements of the tumors.. They used the input images to determine whether a lymph node was cancerous or not by contrasting the feature extraction to preselected thresholds. They made a local feature filter used it as a source images for segmenting the files. Cancer may be detected very accurately using segmentation results of skin conditions.

## 1.3 MAIN CONTRIBUTIONS

In light of the popular research area that targets the treatment of skin bacterial infections, numerous research studies have been published concerning this topic. However, different studies tackle individual deep learning applications and delve into specific aspects of them. Furthermore, even though in the past the majority of research has been focused on the use of supervised learning on labelled datasets, some very recent research starts to incorporate the use of large, unlabeled skin lesion databases.

Given the numerous different factors at play with respect to datasets and techniques, a more global, comparative overview becomes somewhat more strenuous to obtain. This work aims to explore the effectiveness of different supervised learning methods on a limited, labelled dataset, their performance w.r.t. overfitting and imbalanced classes, as well as the use of unlabeled data to improve performance of using Deep Learning and Medical Data Classification for Predicting Bacterial Skin Infection. Thus, we hope to provide a more structured horizontal comparison between different routes for classification and dealing with often-encountered problems in this field. We used CNN and its seven distinct frameworks to evaluate the reliability of photographs of skin infectious diseases and conducted a proper assessment to pick the optimum framework for this issue..

## 1.4 THESIS ORGANIZATION

The Chapter will be organized in such a way that Chapter 1 will include an outline of the thesis and a brief description within each section. The context information and field tasks presented in Chapter 2 will be important to the thesis's subjects. Theoretical outline of the problems addressed in this study will be presented in Chapter 3.. It describes the theory's design as well as the existing methodology for execution and contrast, as well as many post for application. To practice in MATLAB and test the hypothesis approach, a database of Computer Vision and Patient Information Analysis for Forecasting Microbial Skin Disease should be used. This data is displayed as well. This chapter will summarize the summary as well as lab practice, which will be contrasted. The fifth chapter will discuss The study is summarized and concluded in the concluding section. This chapter includes a summary of findings, as well as the thesis's concerns and consequences, as well as a summary of possible studies that may be undertaken more to investigate the topics discussed, as well as a bibliography.

# 2. LITERATURE REVIEW

The ideas put forward by Alan Turing in the midst of the 20th century with regard to the rise of machine learning are increasingly gaining momentum. The (total) Turing Test states that an artificial system can be considered intelligent if it can interact with a human (either in written manner or combined with visual simulations), without the human being able to know the nature of the system (be it a machine or an actual human) . As machine learning becomes thus embedded in our society, with applications ranging from online search suggestions to chatbots, being used for personalized marketing purposes, entering the financial world for stock predictions, etc., it has also managed to make its way into the medical world . For purposes of computer-aided diagnosis and personalized treatment planning, machine learning is treading a clear path forward. Given their current popularity, it is however important to note that these, undeniably powerful, techniques should however be handled with care and understanding, which is even more imperative in the medical world. Therefore, this chapter has as purpose to ease the reader into the concepts of deep learning to improve understanding and point out the critical aspects in dealing with machine learning techniques.

The chapter commences with a brief exploration of general machine learning notions and techniques. In light of the biological nature of the problem, it is interesting to explore the existing synergy in research between the fields of neuroscience and machine learning. This enables us to introduce the concepts of deep neural networks. From this discussion, the need for other deep learning techniques will naturally surface and subsequently be explored. It is natural that given the years of extensive research in these fields and the broad range of topics it enraptures, only a brief representation can be given in this work. Therefore, this chapter aims to introduce all necessary concepts to guide the way towards the applications for skin Bacterial infections. As the goal entails an image classification problem, all concepts will be translated to this level.

## 2.1 CONVOLUTIONAL NEURAL NETWORK

A Convolutional Neural Network (CNN) is a set of algorithms that filters stimuli using convolutional to extract relevant information. A source image map was produced by comparing a feature vectors with a linear combination. To obtain the most helpful data from a given job, the macros are selected depending on learned parameters.. Convolutional networks recognize the right elements of a mission automatically. Computer vision, eventually happen, document interpretation, voice control, data analysis, and other fields have used deep neural networks One input image, one maybe more hidden units, and one output neurons make up a Classifier Model. Thick layer, convolution, grouping surface normalization surface, fixed powerful language coating, fully associated layer, and so on are examples of such sheets. On - network of a Deep Neural Networks, there must be at least one fully connected layer. Figure 2.1 depicts a Recurrent Neural Program's entire architecture.

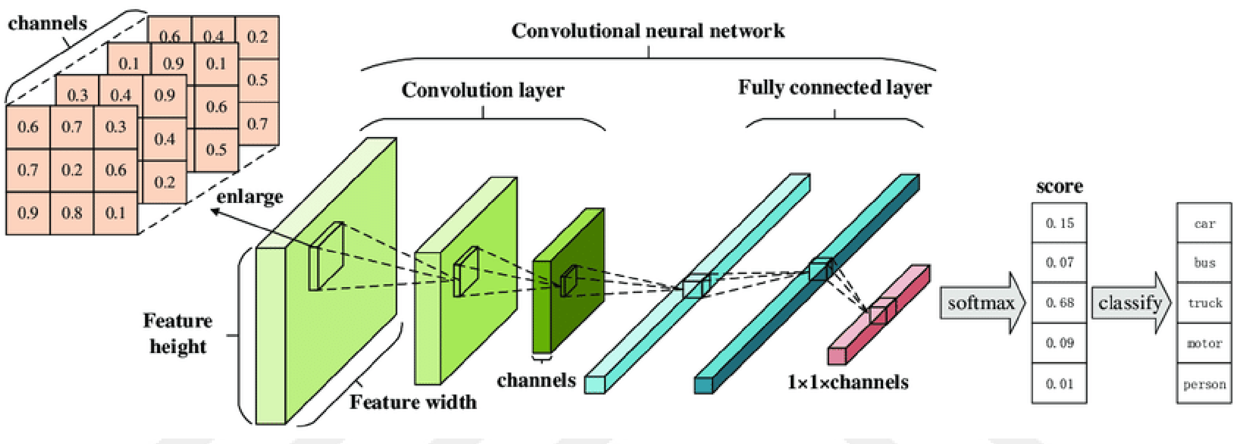


**Figure 2.1:** Architectures of Convolutional Neural Network [13]

### 2.1.1 Input layer

Only digital images is used in CNN's input layer. [width x height x depth], which is a vector of image pixels, are the 3 parts of these images. For instance, for an input of (width=32, height=32, depth=3) or [32x32x3], where thickness refers to the Red, Green, and Blue (RGB) streams,. In addition, the activation function must be divided by two several times. To function with the input nodes, then transform the four structure into a new paragraph. If a picture has the dimensions 32x32=1024, it must be transformed to 1024x1 before being passed into the data. The element of feedback for ‘x' training images will be (1024,x) The information source of a CNN is shown in

Figure 2.2.

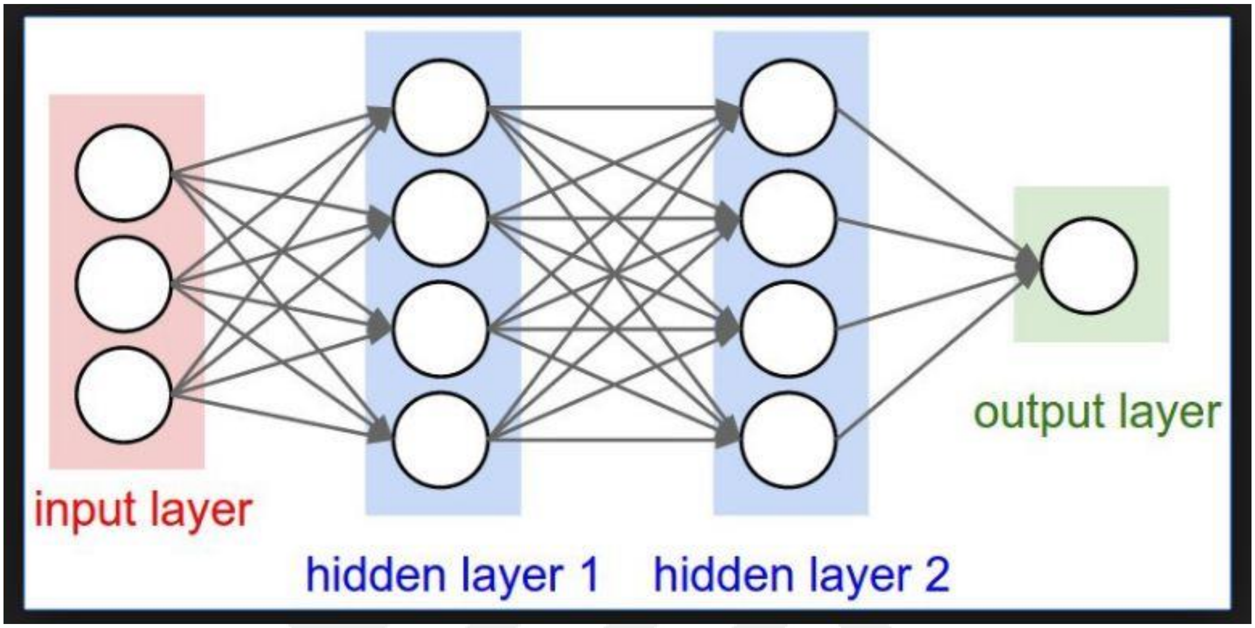


**Figure 2.2:** Input Layer [14]

### 2.1.2 Dense Layer

In a neural network, the thick layer is really a semi surface. Such levels use the same equations as regular surfaces, with the exception that dense layers transfer the end outcome via a semi function known as the Input layer. One of the exceptional characteristics of the thick layer is that it can design some mapping algorithm.. Although there are some limitations for example for any given input vector, the output will always be the same. Dense layer neither can produce different answers on the same input nor can detect the repetition in time. Figure2.3shows the dense layer of a CNN.

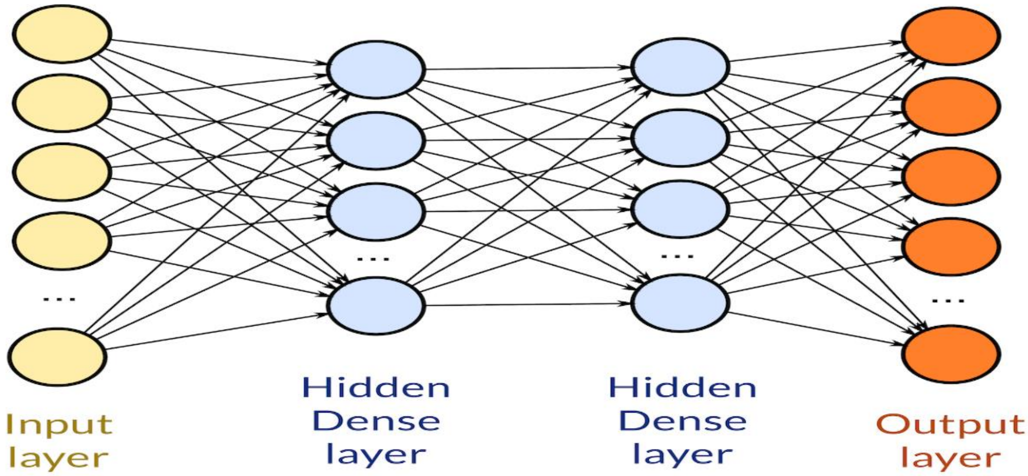


**Figure 2.3:** Dense Layer [15]

### 2.1.3 Convolution Layer

A Convolutional Network's central stepping stone is the Convolution, which handles the majority of the computational efforts. The fully connected layers system includes filtering to create certain variables and classification algorithms from which it extrapolates and knows.. In a sentence, this is a feature extractor layer. Input images are compared with segments to find out the changes. These segments are known as features. This layer selects one or more features from the input images and creates one or multiple matrix and dot product with the image matrix. It also calculates the output neurons connected to the local regions. Furthermore the whole computation gives out a result known as the convolution layer. For a given I x I image size and F x F filter size, the convolution result will be:

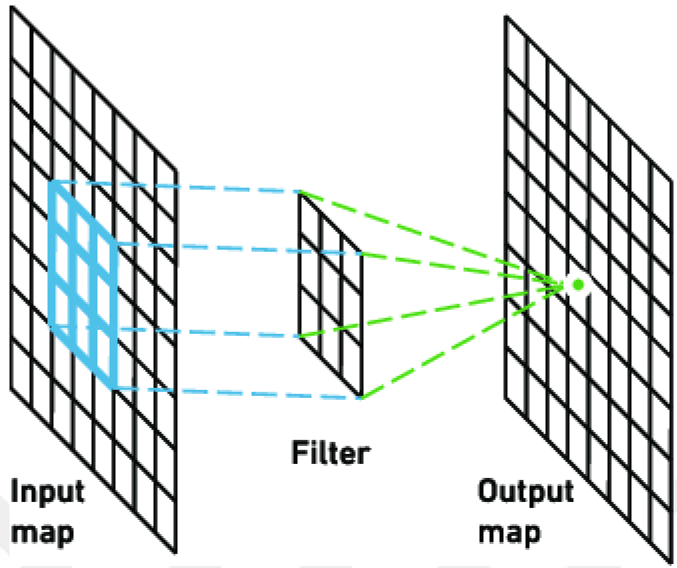


**Figure 2.4:** Convolution Layer [16]

### 2.1.4 Rectified Linear Unit Layer

The artificial neuron of the Rectified linear unit (ReLU) layer is a cost function vector quantity which will emit the useful results immediately unless the feedback is good, or else it will produce zero. When the product of the convolution is passed to this surface, it will shift all the significant figures to zero while leaving the bigger value alone.. Many forms of biological systems now use ReLU as their standard complex formation. Model initiated with ReLU can be trained easily and also it achieves better performances. ReLU layer does not have any parameters or hyperparameters. Figure2.5shows the rectified linear unit layer of CNN model.

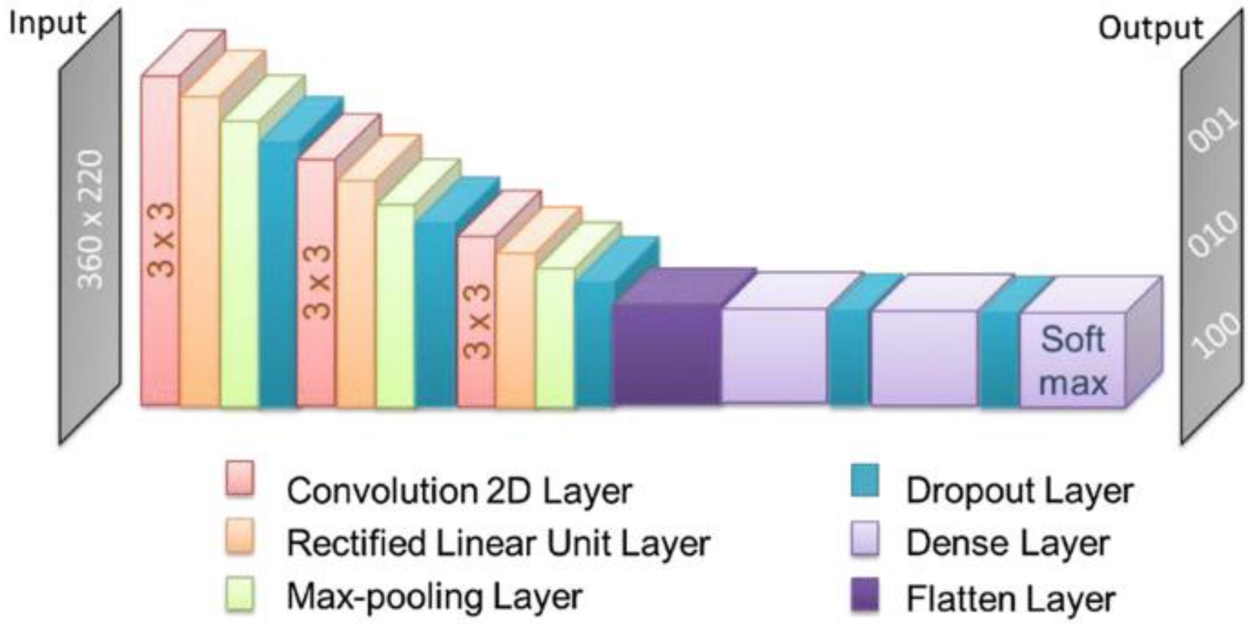


**Figure 2.5:** Rectified Linear Unit Layer [17]

### 2.1.5 Pooling Layer

The pooling layer is a component of a Convolutional Neural Network that functions to minimize the representation's model complexity in order to reduce the number of inputs and computations in the process. Since the max pooling is not reliant on the accessibility or amount of apps in the system, it can operated separately from each input image. The most popular implementation used in pooling is known as max pooling. Pooling layer does not have any parameters but it has additional hyperparameters: Filter(F) and Stride(S). If the input dimension is X1 x Y1 x Z1,

Figure2.6 shows the pooling layer of a CNN model and the max pooling mechanism.

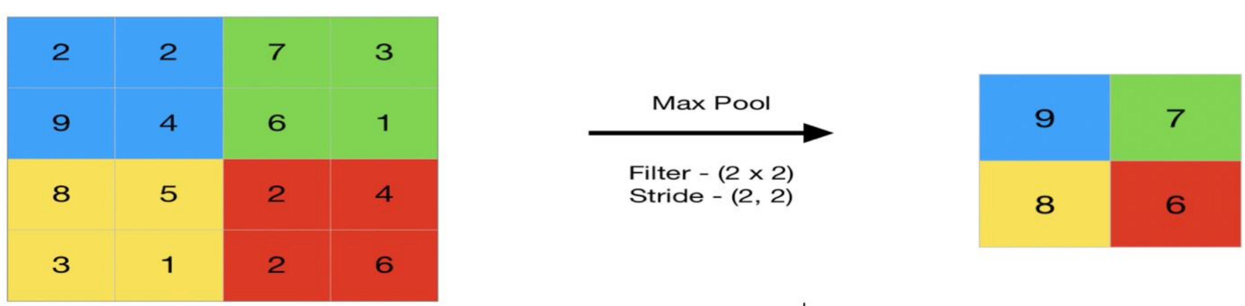


**Figure 2.6:** Pooling Layer [18]

### 2.1.6 Normalization Layer

Normalization layer basically normalizes the activation outputs of previous layer which means it puts in a transformation that upholds the mean activation close to zero and the activation standard derivation close to 1. Batch normalization is mostly used here although there are many other alternatives like weight normalization, layer normalization, instance normalization, group normalization, spectral normalization etc. Figure2.7 shows the normalization layer and various normalization methods.

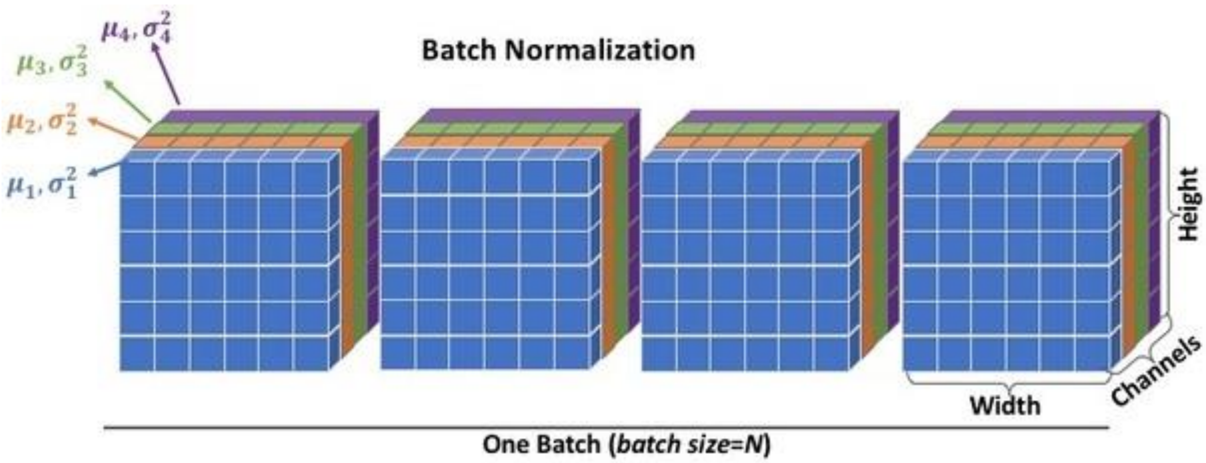


**Figure 2.7:** Normalization Layer [19]

### 2.1.7 Fully Connected Layer

In most cases, a fully connected layer takes input quantity and emits a N-dimensional matrix, whereby N represents the size of groups selected by the programmed. The data amount is derived from the matrix multiplication, Relu, or pool surface performance.. After analyzing the outputs of the previous layer fully connected layer distinguishes the mostly matched features of a particular class. Fully connected layer works on features which are high level and have particular weights. In this way fully connected layer calculates the odds for the different classes as it calculates the product outputs of the weights and the previous layer. Figure2.8 shows the fully connected layer of a CNN model.

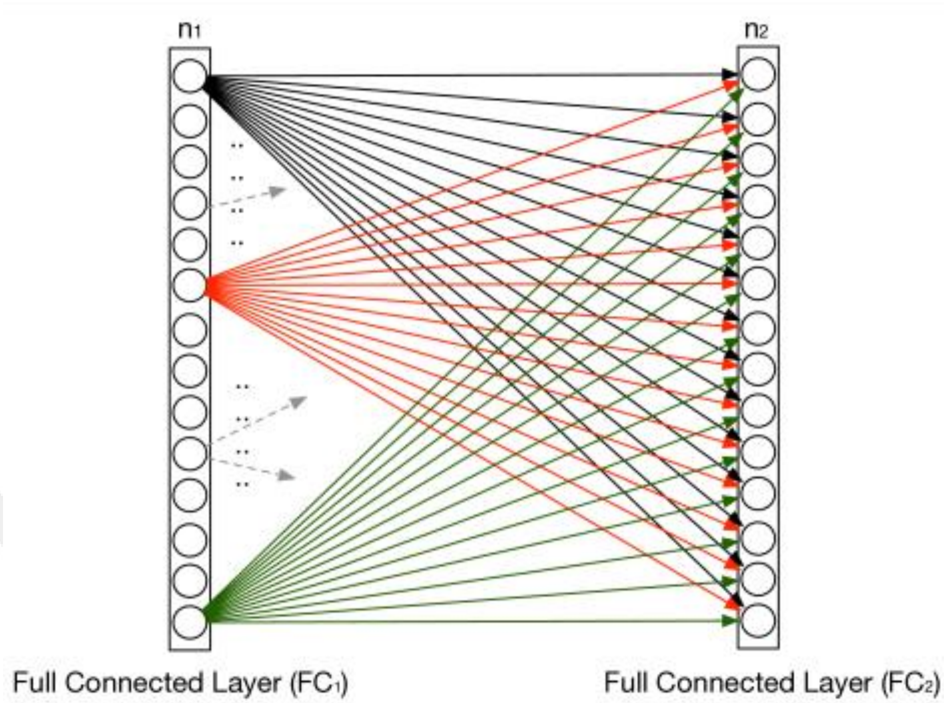


**Figure 2.8:** Fully Connected Layer [20]

### 2.1.8 Output Layer

The activation function is the last layer in CNN and it generates the project's correct outcome. The output unit neurotransmitter specification is frequently changed in order to comprehend the outcome as well as the entire programmed.. After all of the data has been adequately trained as well as the measurements were registered, it will compare the output to the train set and decide if it fits or not. The outer part in a statement condenses and accurately generates the outcome. Figure2.9 demonstrates the performance or the ultimate surface of a CNN template.

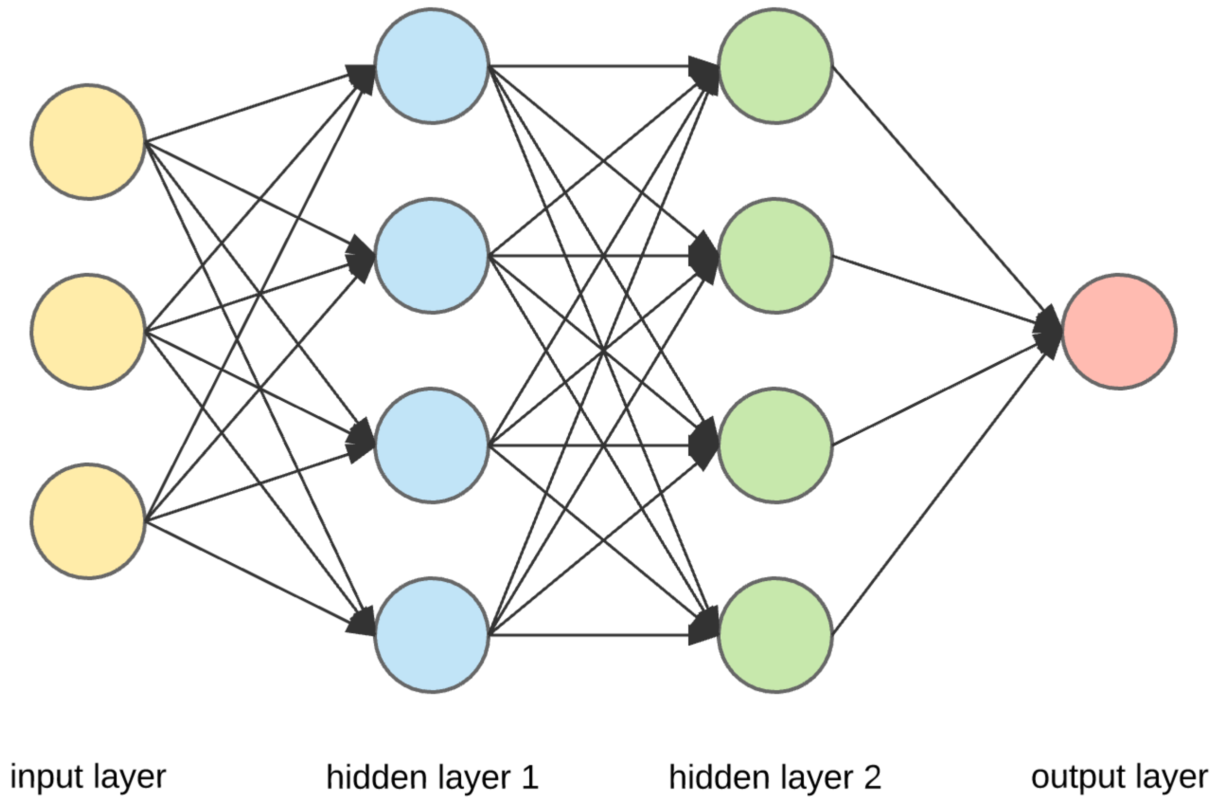


**Figure 2.9:** Output Layer [21]

In this way, CNN takes, process, trains and thus predicts for the given inputs.

## 2.2 NEURAL NETWORKS

Neurons form the structural building blocks of the brain and can be considered as the primary information carrying units. The pyramidal neuron depicted in Figure 2.10, shows the three main neuronal components: the dendrites, cell body and axon. Information flows along the neuron in the form of an electric signal, known as the action potential (AP). The neuronal membrane with a resting membrane potential of a value ranging from -90 mV to -40 mV depending on the type of neuron, gets depolarized by a sodium influx through voltage-gated sodium channels. Upon reaching the action potential threshold, often between -50 mV to -40 mV, an explosive influx of sodium occurs, followed by a repolarization due to a potassium efflux through slower-responding voltage-gated potassium channels [29]. These ion currents are driven by their electrochemical gradient. A refractory period is kept in place by the inactive state of the sodium channels, during which they will not respond to depolarization, thus preventing the signal from traveling backwards.

The passing of an AP (nerve impulse) is referred to as the firing of a neuron. As a consequence of the way AP's are created, they are all equal and independent of stimulation strength. Information on the type of stimulus the neuron receives is instead encoded in the neuronal firing rate, with stronger impulses leading to higher frequency of action potentials [30].

Communication between different neurons is enabled by synapses, either electrical or chemical, the latter being the most common type and discussed here. In response to a depolarization, the pre-synaptic terminal will release neurotransmitters that are contained in presynaptic vesicles into the synaptic cleft by exocytosis. The neurotransmitter subsequently diffuses across the cleft and by binding to specific receptors, the neurotransmitters can incite a change in the postsynaptic membrane potential, thereby allowing the dendrites to receives information. Two of the most common types of neurons are the excitatory neurons, releasing glutamate and causing a depolarization or excitatory post-synaptic potential (EPSP) and inhibitory neurons releasing GABA, which cause a hyperpolarization or inhibitory post-synaptic potential (IPSP) [31].

Neurons generally receive their input at the dendrites, which are often covered with small appendages, known as dendritic spines. A pyramidal neuron in the CA1 region of the hippocampus has over 30 000 dendritic spines through which it may receive input from other neurons [32]. This physiological hallmark underlies the ability of the adult human brain to adapt. Through the formation of new dendritic spines, which may receive neurotransmitter through volume transmission or can connect to other neurons, thereby creating new synapses, or adaptation of existing spines in response to e.g. high-frequency stimulation of the pathway, plasticity in the human brain is enabled [33].

The presence of such large numbers of input-channels portrays the need for a strong synaptic integration process. Electric signals generated at postsynaptic terminals will spread along the membrane towards the cell body and eventually the axon hillock. Due to the behavior of cell membranes as an RC-transmission line, the passive diffusion will distort the signals. Furthermore, the individual PSP's generated at the numerous postsynaptic terminals are most often in the subthreshold range. In light of the large number of connections however, they are very likely to sum together in either time or space, thus evoking larger changes in the membrane potentials [34]. This summation of signals that were distorted due to their travels along the dendritic arborizations provides the means for neuronal information-integration [35]. As the main dendritic branches come together at the soma, this is were the final integration takes place. Subsequently, the signal goes to the axon initial segment (i.e. axon hillock), a region characterized by a high sodium-channel density. The corresponding local decrease of AP-threshold renders it a favored region for action potential initiation.

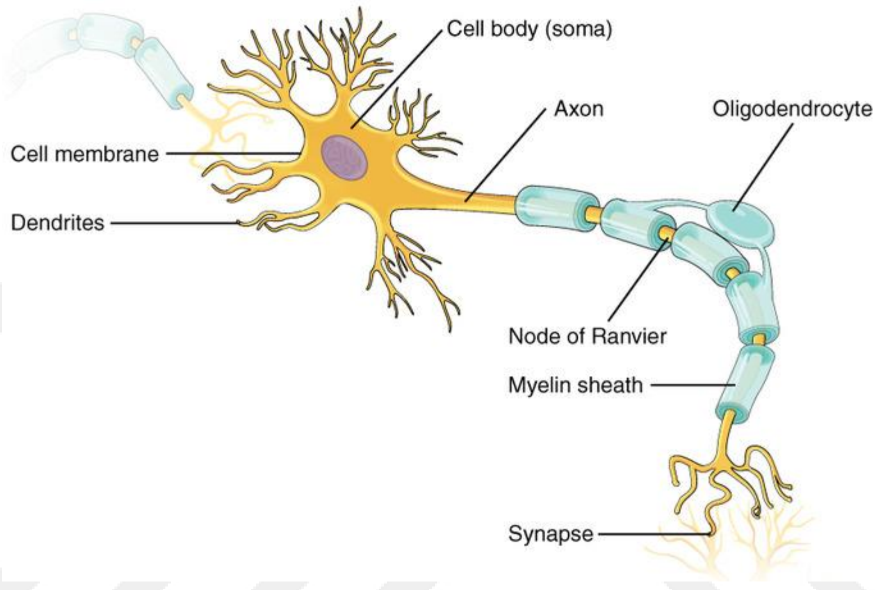


**Figure 2.10:** Structure of a neuron with a detailed view of synaptic transmission [22].

## 2.3 FROM THE VISUAL HIERARCHY PATHWAY TO CNN'S

To overcome the problems encountered in the field of computer image recognition, further inspiration was drawn from the concepts of human visual perception, which has lead to Convolutional Neural Networks (CNN's).

Biological visual perception was classically considered to occur through two separate retino-cortical pathways. The existence of a 'what'-pathway and a 'where'-pathway was observed after the Second World War in veterans with cerebral missile wounds by Newcombe & Russell . Lesions in the parietal lobe impaired the maze-learning performance of the patients, whereas lesion in the temporal lobe resulted in a decreased closure ability, i.e. mentally reconstructing an image based on incomplete information. Further evidence for this model was acquired in a study by Ungerleider and Mishkin in which macaque monkeys were impaired with focal lesions in the cerebrum and investigated on an anatomical and electrophysiological level . Their results indicated a distinction between two pathways originating from the primary visual cortex V1: a dorsal pathway projecting to the posterior parietal lobe and inferior ventral pathway to the temporal lobe, which are respectively involved in the visuospatial and subperceptual functioning of biological vision , as illustrated in Figure 2.11.

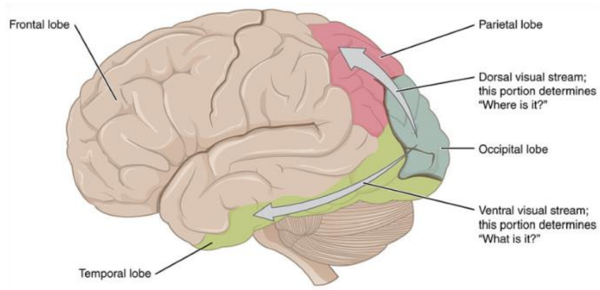


**Figure 2.11:** Simplified depiction of the two visual streams [23]

As indicated in Figure 2.12, both pathways receive their input from the photoreceptors at the retina and pass through many of the same cortical areas before parting ways spatially. They are however segregated on an anatomical level from as early as the ganglion cells on the retina, which is reflected by the two pathways synoptically mapping at different layers in the same cortical areas they cross. At the lateral geniculate nucleus, the visuospatial system springs from larger neurons at the ventral side and is correspondingly known as the magnocellular-pathway, which processes luminescence-based spatial inputs. Contrarily, the parvocellular-pathway, which refers to the subperceptual system stemming from smaller neurons at the dorsal side, conveys color-sensitive input without regard to spatial aspects.

Further distinctions can be made between the pathways with regard to their required outputs. The dorsal pathway projecting to the parietal lobe conveys the information required to execute an action, i.e. a spatial description of the scene (position, orientation and structure), which is supported by the high temporal sensitivity of said pathway. The posterior parietal lobe receives input both sensitive to the spatial scene of objects and self-initiated movements, correlating the body’s position to its surroundings and it further projects to the frontal lobe, where it thus plays a role in reaching movements of limbs and hand and finger grasping actions, as well as ocular control. The ventral pathway on the other hand provides higher-resolution information more slowly to the temporal lobe with detailed perception as objective. The structures involved in the ventral stream play a role in visual perception, memory and learning.

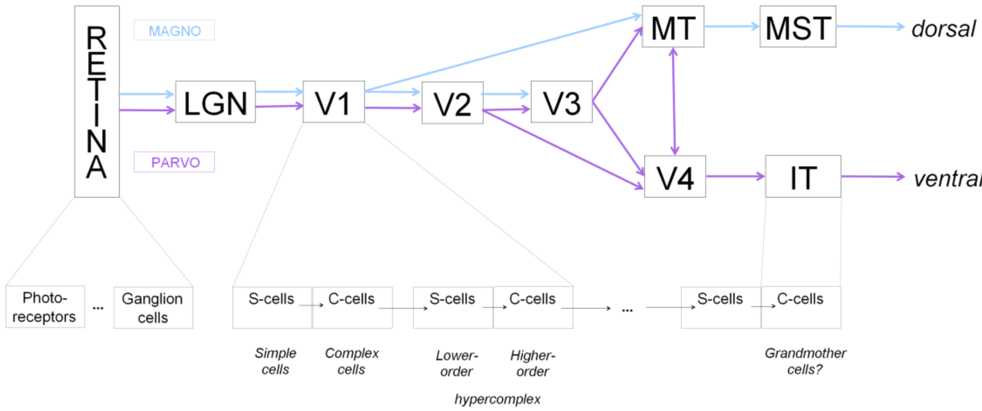


**Figure 2.12:** Comparative illustration of the organization of the two visual pathways and the stacking of S- and C-cells [24]

## 2.4 OBJECT RECOGNITION IN THE VENTRAL VISUAL PATHWAY

In the 1960s, neurophysiologists D. Hubel and T. Wiesel made important observations about physiological computer vision by providing insight into the workings of the dorsal stream. Centered scissor blades of illumination were found to be the most efficient in activating some red pulp cortical nerves in their studies with animals., An directed line of specular reflection, on the other hand, was more efficient in activating nerves in the nucleus accumbent and, as Koffler [REF] already demonstrated, nerves in the hippocampus. This revealed the variations in vision between the periphery and the cortex, as well as the potential significance of inhibition factors influencing sensory neuronal' temporal information. Second, they defined the sensory cortex's bathymetric framework, i.e., retinal vision mapping are depicted in different map data throughout the cortical, with hexagonal maps representing neurons storing a same details. Finally, they discovered a hierarchical system in the sensory pathway's cell organization. Big data was thought to be linear via this series of massive more specialized animals, identifying basic, linear, reduced, and greater strategy was launched cell types.. More complex cells have been less responsive to line location, were assumed to depend on knowledge transfer, and tended to have wider application areas because they did not reply as strongly to a line of specular reflection. Hubel and Wiesel demonstrated hierarchical cognitive processes in the occipital cortex V1 by different types of cells characterized by their convolutional layer and resistance. They also hinted at the presence of related neuronal forms in other areas of the visual cortex (V2, V3 and V4). Finally, cells in the inferotemporal cortex can deal with increasingly dynamic trends even though the picture is changing rapidly. Taking a break from the traditional two-stream, feedback control conceptual picture: Any recent developments As we progress from basic science, it become clear that, like any physical method, biochemical sight is not as simple as it appears. On a research emphasis, it's worth noting that the two paths aren't entirely distinct. Not only does the dorsal stream need input from the ventral stream to complete every vision - spatial mission, but current research suggests that perhaps the two rivers communicate along route as well. L. Cloudman addresses three potential forms of cross interaction in her work, and recent studies using diffuse mri feature selection algorithm during hand activities recorded bridge through unique white pass routes linking two channels. It is vital to know that a simple feedback control design not encompass the complexities of sensory acuity on a vendor site.. Through identification of an object seen in a time span of 100-200 ms (i.e. ‘blink-of-an-eye' timeframe), centralized feedback control representations have the high ground throughout the dorsal stream, only with goal of transforming energy to a neural expression in the sabotaged cortical. Powerful input relations play a role as the view period gets longer, enhancing understanding by incorporating finer information gathered at lower tiers of the pathways. As a result, a dynamic interrelationship of adaptive control and guidance interactions in the dorsal stream is suspected to occur for conscientious computer vision on a longer timeframe. Third, the distinction between basic, active, and need any neurons is more complicated than commonly thought. Rush et al. discovered that V1 neurons show various polynomial filter configurations, probably indicating that static and dynamic cells are only two of several potential neuron convolution layer combinations Image recognition driven on by psychology Motivation for machine learning has also been identified from a confluence of things described above. The central biological concept was that the dorsal pathways attempts to turn image data via a number of steps it into lightweight, concise, and separate depiction, irrespective to nonparametric data.. Relying on the feedback control transfer throughout 'eyesight,' the concept of a hierarchical structure arose, with the aim of incorporating the cells' - specificity but resistance behaviors. To accomplish this, opposing types of peptidoglycan that represent the corresponding behavior in prototypes have been created to imitate the concept of static and dynamic bacteria located in V1.

Noncognition at Fukushima Fukushima engineered the initial synthetic neuronal network to do this in 1980.The multilayer neural net consists of alternating layers of S-cells and C-cells These variations, with each S-C pair identified as a point, derive progressively more complex functions from their input, as shown in Figure 2.13. Purpose of service organized associations among cells on input layer ensure the cortex's hexagonal pattern recognition framework, i.e. neurons can accept feedback from a small region of the preceding stage.. Visual perception in people, which relies on complex visual field for the identification of predictable styles at multiple places in photographs, provided additional scientific motivation. Cells fields were created for each surface of the neuron to reflect a community of purpose of service structured neurons obtaining the very same collection of inbuilt functions.

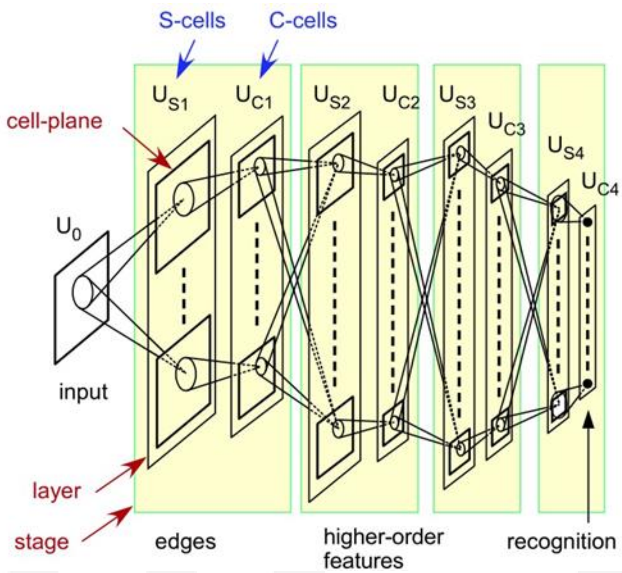


**Figure 2.13:** General architecture of the neocognitron [25]

In this architecture, the S-cells are responsible for feature extraction, where the features to which they will respond are determined through a learning process of the variable input connections. Simple features, such as specific orientations of lines and edges, will be extracted by lower-level S-cells, while higher-level S-cells extract more global features (e.g. parts of learned patterns). The C-cells receive their inputs through fixed connections from S-cells in the previous layers and are responsible for a robust pattern recognition (i.e. decreasing sensitivity to a deformation or location shift of a pattern). Each C-cell receives inputs from a number of S-cells ('the input window') in one cell plane, i.e. from S-cells that extract the same feature, but at different spatial locations. The C-cell will fire, if it receives an input from at least one of the S-cells. Consequently, the feature will be detected even under a shift in the location of the input features, rendering the system less sensitive to the exact feature locations. The behavior of the C-cells can however also be interpreted from an alternative point of view. The input windows for the different C-cells strongly overlap thus C-cells can be considered as performing a spatial blur on the excitatory signals they receive from the S-cells. This spatial pooling is obtained by averaging these signals from the input window, which are S-cells that perceive the same feature at slightly different locations. Furthermore, the excitatory S-cell input window is often framed by a small inhibitory region. This enables the C-cells to distinguish a continuous line from the end-point of the line and allows the network to still recognize features after blurring. A consequence of the fixed input windows of the C-cells is a reduction in size of the cell-planes, thus allowing the network to compress data as it progresses to higher stages.

## 2.5 AUTO-ENCODERS

CNNs in particular rely on supervised learning, with backpropagation of the error throughout the net. However, the question arose in the past as to how to learn an internal representation without the availability of target outputs. Thereto, the structure of auto-encoders (AE) was suggested, which aims to use the input as target output, exploiting error backpropagation to achieve an optimal 'mirroring' of the input.

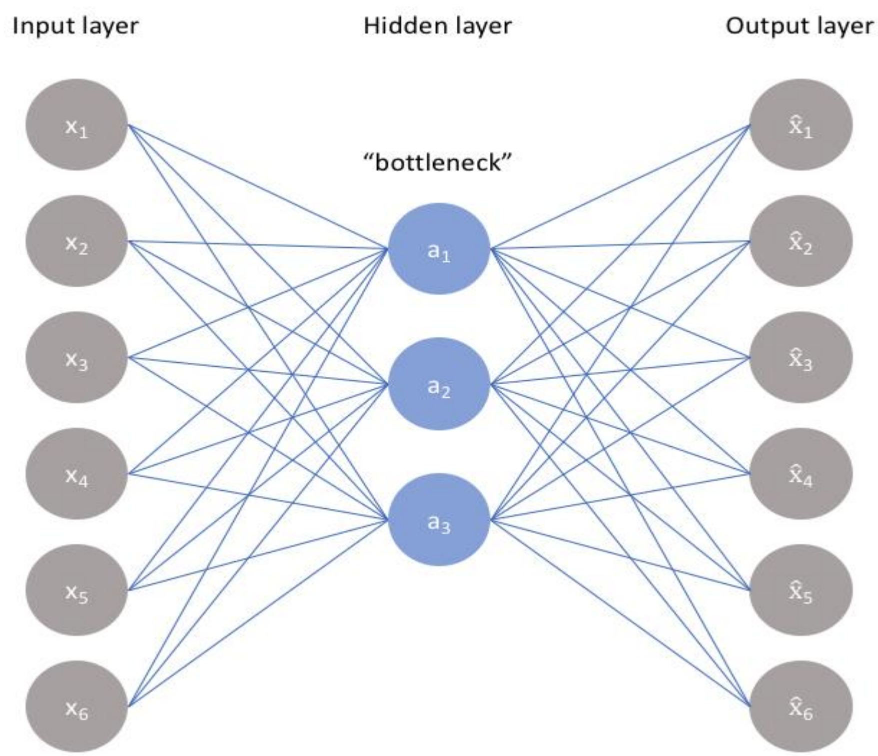


**Figure 2.14:** Architecture of an undercomplete auto-encoder building block. The fully-connected autoencoder contains a single hidden layer of lower dimensionality than its input layer [26]

### 2.5.1 Deep auto-encoders

The importance of auto-encoders has also surfaced in deep learning. Originally done by stacking several auto-encoders on top of each other and training them in a consecutive bottom-up manner to learn the subsequent stages of internal representations, the trained encoder can be singled out. Subsequently, stacking a top-model on this encoder gives rises to a deep neural network that has been partially pretrained . It thus exploits the use of unlabelled datasets for 'kick-starting' the supervised training of deep architectures. The use of pretraining a neural network has been suggested to act as a regularizer, giving rise to the starting point and restricting the parameters of the optimization process during supervised learning to a specific, favorable parameter space. When expanding the depth of encoder and decoder, both are in essence feedforward neural networks and can thus alternatively be trained with backpropagation and gradient descent.

The use of a deep AE for pretraining can also be extended to applications of image classification. In this regard, stacked convolutional auto-encoders have been proposed as alternative to random weight-initialization of a CNN. This architecture allows for unsupervised pretraining of a CNN-base model, followed by supervised learning of the top model and finetuning of the base model weights.

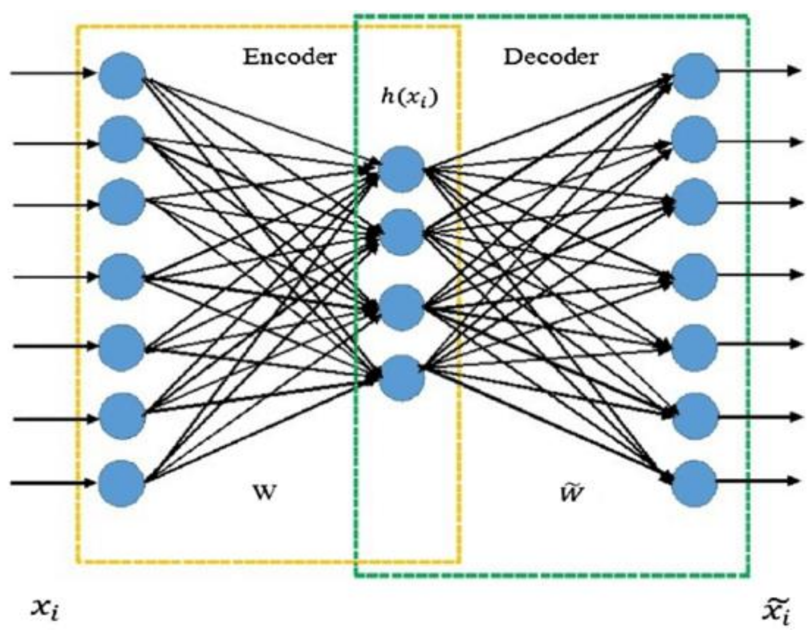


**Figure 2.15:** Architecture of an overcomplete auto-encoder building block [27]

## 2.6 ROLE OF DEEP CONVOLUTIONAL NEURAL NETWORK TO PREDICT SKIN BACTERIAL INFECTIONS

Researcher in proposed a methodology that used a pre-trained DNN to spontaneously detect the features which can later be used to find out Bacterial skin diseases dataset. Their out put results succeeded the current existing DNN based architectures. The main part of their system was a pre-trained CNN architecture to extract features from their dataset. Their aim was to create a CNN architecture which can be determined by various factors such as the type and the size of the dataset as an alternative fine tuning technique of CNN. Since their dataset was slightly small, they constructed a classifier model on above of the out result of the hidden layers. The classifier is built with the values of the activations from previous layers of the network. Their proposed technique performed better than employing hand tuned features. Additionally, it was very fascinating to observe that, even though the CNN has been trained with different datasets each time including the datasets that are not related to Bacterial skin infections performed very well to extract features. The reason it performed so extraordinary was that, it could change the skin infections tones because of the lighting conditions.

Researcher in this research established a linear classifier, trained on features extracted from a convolutional neural network pre-trained on natural images, differentiates between up to ten skin bacterial infections with a greater accuracy. Their methodology needs neither lesion segmentation nor complex pre-processing. They achieved a satisfactory accuracy over 5-classes with visible progresses in accuracy for underrepresented classes. Their technique attained a great accuracy outperforming the accuracy for- merely reported. This was an effective methodology to calculating features over dissimilar spatial locations as it reprocesses the conjoint convolutions done previously in the network and can be used to calculate features over multiple scales. Combining features over the spatial dimensions has presented to develop predictive presentation and the resulting feature vectors simplify well to other natural object image tasks.

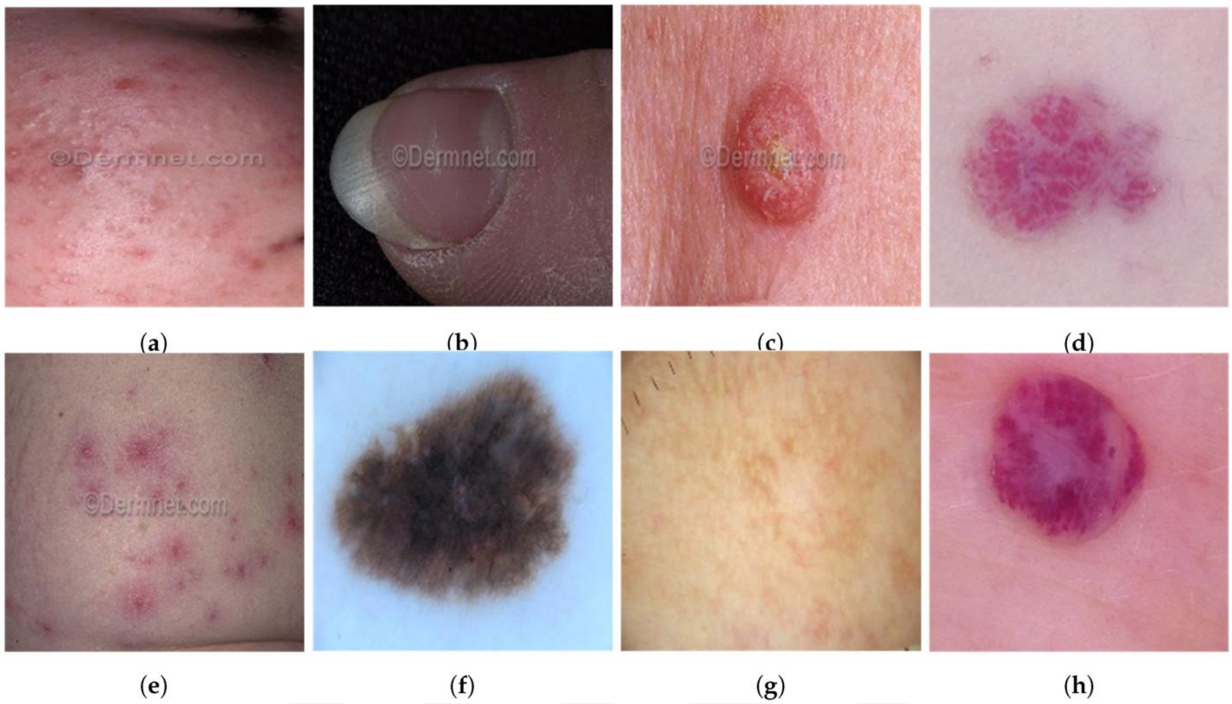


**Figure 2.16:** Examples of correctly and incorrectly classifies diseases. (a) Correctly classified ACROS in DermNet (b) Correctly Classified NAIL in DermNet (c) Correctly Classified SEB in DermNet (d) Correctly Classified VASC in ISIC (e) CEL Misclassified as ACROS in DermNet (f) Correctly Classified AKIEC in ISIC (g) BKL Miscalssified as MEL in ISIC (h) NV Misclassified as VASC in ISIC [28]

# 3. METHODOLOGY

The final exam of such a research has been addressed, beginning with how we resolved the question to construct the system and then extracting our database into a format and can be used with our newly developed system. To begin, we've seen a picture of our current plan so that you can get a good idea of how we're going to be doing. The database summary follows, which describes our database and what it contains. Then, our database post methods, as well as the compilation procedures, were demonstrated, along with a description of all the variables that are being used to compilation our template.

At the start of our project, we gathered our data. On Mysql Database, we finished all of our research. As a result, before anything, we've exported the resources we'll have to finish our project. Our express and check photos already were saved in separate files. Then we post our solutions to achieve our requirements.. Then, using our dataset, we developed and ran a CNN model to see how accurate it was. Then, after breaking the datasets into three folds, we built and ran CNN models with KFold architectures three times, per period using one of the three breaks as a testing package. Then we calculated the accuracy of the proposed model and transferred it to disc. After that, we take various Neural networks with same parameters to find out and forecast the precision in possible to correlate the end outcome. To find the right model for our dataset, we ran ResNet50, VGG16, InceptionV3, VGG19, and Xception architectures. Our control framework is depicted in

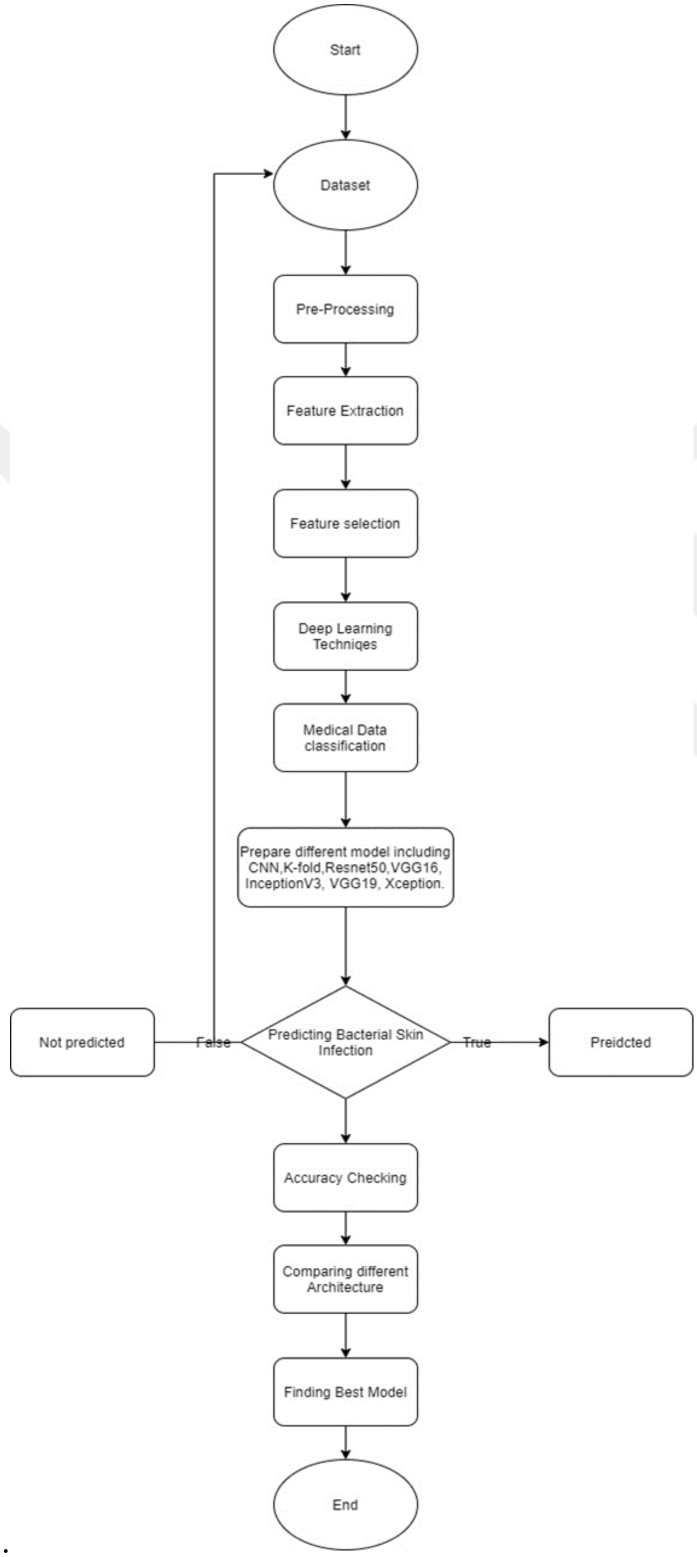


Figure 3.1.

**Figure 3.1:** Flowchart of the Proposed System

## 3.1 DATASET DESCRIPTION

The kaggle application was used as a secondary dataset. Skin infections and Microbial Infections: Malevolent vs Harmless" is the name of the report. A healthy set of photographs of Microbial Severe Infection as well as other skin diseases is included in the database. It has a maximum of 3300 images. ISIC-Archive provided the data for this database. The separated into multiple key files called \test"(660 pics) and \train"(2640 pictures) each with in the directory getting 2 further sub folders named \malignant" and \benign". The train>benign, train>malignant, test>benign, and test>malignant directories contain a total of 1440, 1200, 360, and 300 images, each. There are photos in each of the files mentioned, with its own special name. For the KFold architectural design, we divided the entire model train into three divisions and used one of them as a verification divide three to four times. Figure 3.2 displays thinking " of our repository.

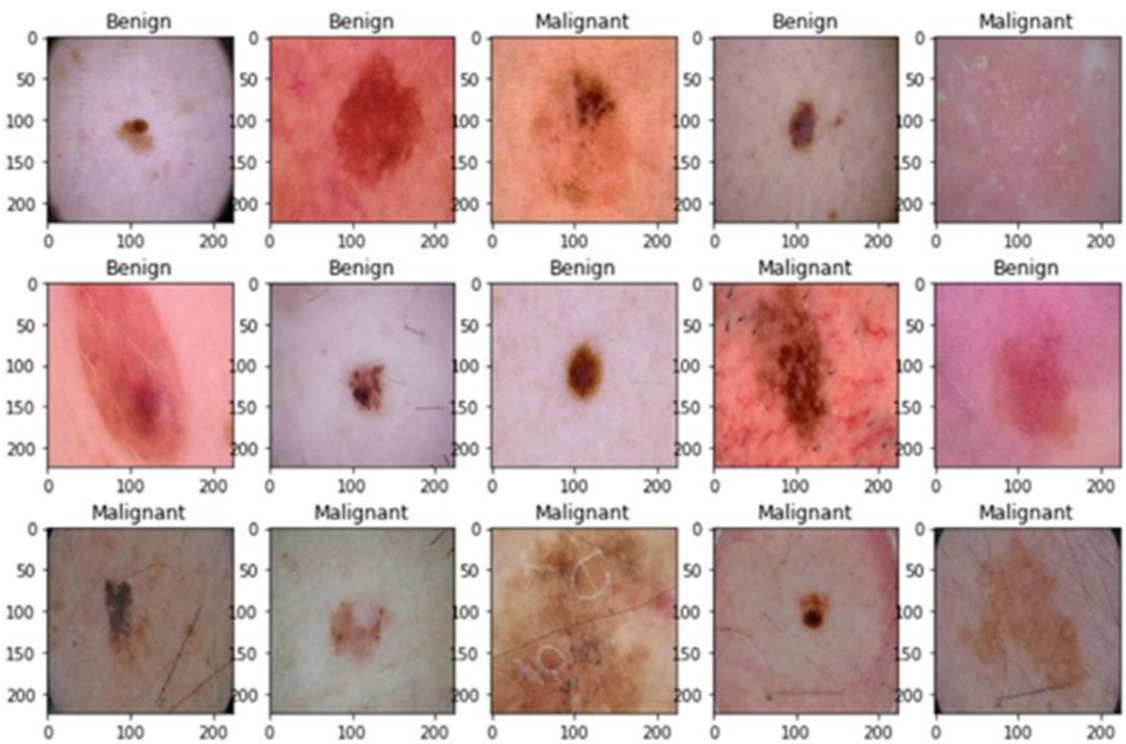


**Figure 3.2:** Sample Images from our Dataset

## 3.2 IMAGE PRE-PROCESSING IN MATLAB

All of the photos in our database have same width of 224x224 pixels. We read all of the pictures as a page of modules initially, after which decided to convert them to Rgb. Then, for each of us, we translated the collection of ranges with the html element uint8." We marked the healthy objects as 0 or cancerous objects as 1. We have computed both healthy and diseased photos from of the training set and testing directories into two separate arrays called training set and testing collection. As part of the normalisation, we categorised this same test and train inverters by 255 to ensure that all values remained within the same range of 0 to 1, with closer to 1 indicating malignancy and nearer to 0 indicating benignity.

**Compiling Model**

We operated on compilation the template after finishing the window is located. As a method of data post, the edge map of an image features from the database has become 224X224X3. We experimented with a range of instructional rate for our template and discovered that 1/ 103 produces the best results.. Our products are divided into three types. Furthermore, we was using the ‘relu' feature as an input signal and ‘david' as just an optimization method. We use ‘numeric' as our weight vector and de ned ‘precision' as ours metric before the end when assembling that template. Finally, we was using a feature called 'educational reductions.' If the quality of the training data continues to fall below 1/107, the linear function must be balanced. We completed that compilation template phase while also running the various Neural networks.

**Weight Selection**

In our study, we used the proportions zero. Other choices include using post scales or driving to the weigh station and filling the scales. Instead of starting from the beginning to validate the system so that it could learn on its own, we compared each template to perform classification for this venture..

## 3.3 POOLING LAYER SELECTION

In our design, we use Max Pooling 2D for the pooling layer. There are many forms of residual blocks possible but even among these peak accumulating and batch normalization seem to be the most popular and most commonly used. If we ever need to finding additional across the given dataset, pooling is a wiser alternative because it uses the device's mean amount from the de jon vector. However, since we are identifying diseases from a physician's part of the body that is just a part of the entire picture, we should use maximum merging. Furthermore, max pooling is a better alternative here as it removes the picture's strongest characteristics. It removes its most significant features, such as template borders, while loss function removes characteristics in a more fluid manner. Keras defaults to a pool size of 2X2 and a strides function of 2 if no variables are defined. Even so, we chose a sampling rate of 2X2 for the sake of code usability. Pooling layer would receive the maximum value of each pixel from a matrix format and substitute it with a tiny dot for the spatial domain..

### 3.3.1 Dropout Selection

Slacker is a supervised classifier used in CNN to avoid the database under question during the training period. What dropout does is it reduces the difficulty of the template by the specified price of dropout. Dropout aids in the extraction of even more advanced tools from a computer program thus increasing practice time.. We used 0.25 as the high school senior price in our design. That is, it will miss 25% of the nerves at random during preparation. The drop out value varies from application to application, depending on how a problem is solved. We experimented with various drop - outs rates to see which produced the best results, and we discovered that 0.25 is the best.

### Activation Function Selection

In an algorithm, the validity criteria receives an input from a prior node, analyses it, and generates a result for that same nerve cell, which is then used as source in the next nerve cell. There are a variety of control optionsThat being said, we only used two forms of hidden layers in our current plan: the Sigmoid and the Relu. Operate.

The more pessimistic the output, the nearer the performance is to zero in a sigmoid equation. Similarly, the better the results number, the close the performance would be to 1. From 0 to 1 will be the distance..

$$S(x) = \frac{e^x}{e^x + 1}$$

Figure 3.3 shows the sigmoid curve for any input.

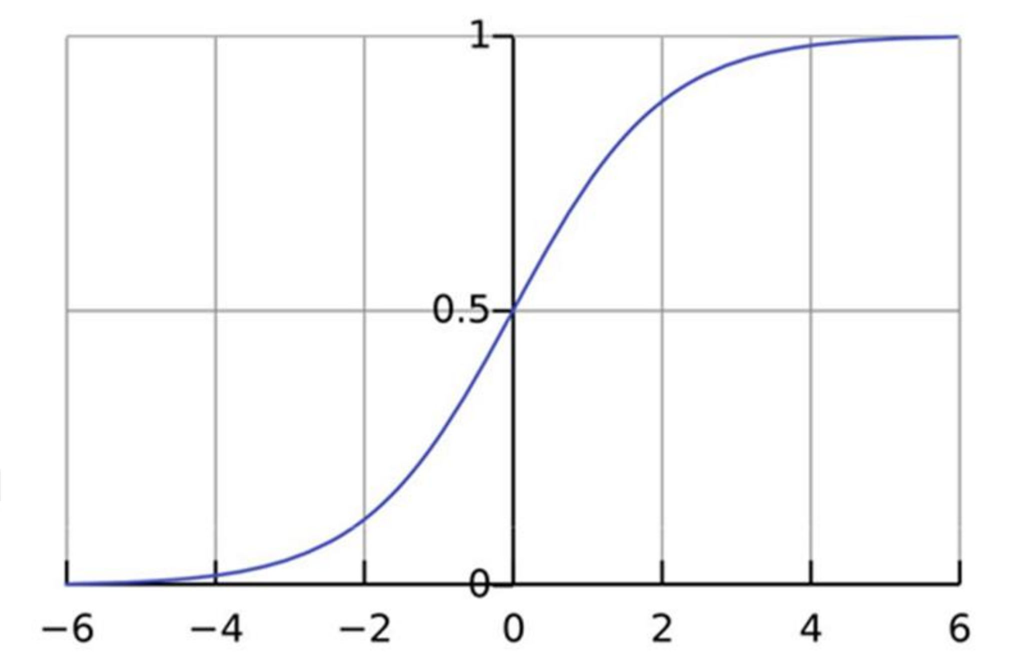


**Figure 3.3:** Sigmoid Function

Softmax Layer Feature: A type of sigmoid function that can be used in classification tasks is the Soft - max input image. Two groups can be handled by a standard sigmoid feature. But what if we have to deal with many courses? The softmax feature then comes to the rescue. The softmax process uses each class's performance into a value of 0 and 1..

Relu Function: A Relu function translates a number to the a scale starting at 0 and ending at infinity. In other words, if the input is below or identical to 0, the cost function would be 0. In addition, if the voltage is higher than 0, the value will be the price.

$$f(x) = \max(0; x)$$

Figure 3.4. shows the relu curve.

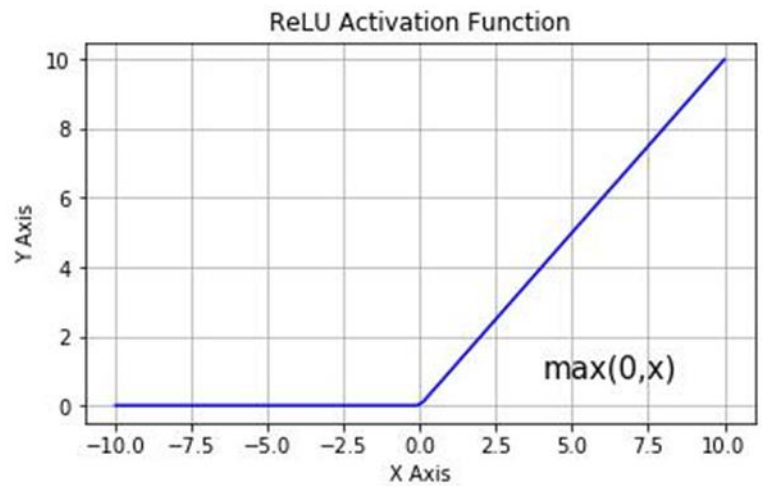


**Figure 3.4:** Relu Function.

# 4. RESULTS

The whole implementation procedure of our model have been thoroughly discussed for Predicting Bacterial Skin Infection using Deep Learning and Medical Data Classification. We have used CNN with KFold along with 7 o A Relu function converts an amount to a measure that starts at 0 and goes all the way to eternity. In those other words, the functional form is 0 if the feedback is less than or equal to 0. Furthermore, if the energy is equal than 0, the price would be the cost. Using Matlab, we trained and tested our database and use other Cnn models (ResNet50, VGG16, VGG19, InceptionV3, Xception, etc.). Each segment begins with a description of the prototype, followed by the variant we used it to practice our method of that structure. Eventually, photographs from our research were used to explain how we used particular systems and the criteria that we used. Integrated delivery for every 5 periods in each segment until 50 iterations have been seen with their loss, reliability, val-loss, and val-accuracy. Then, together with some comparison testing set of our datasets and the expected outcome of the use frameworks, a comprehensive schematic description (Precision vs Time periods curve and Loss vs Epochs graph) of each design of the analysis results was displayed, and even some exam objectives photos from our database and the projected outcome of our using frameworks were contrasted to display a comprehensive systematic review.. A review of two CNN models of their reliability and failure can be shown with a graphical visualization at the conclusion of the study to evaluate the frameworks further accurately.

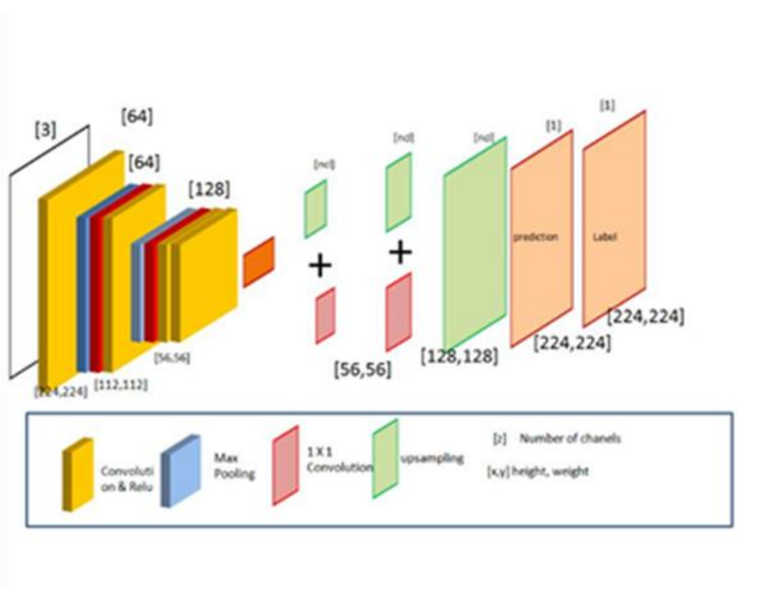


**Figure 4.1:** CNN Model

## 4.1 BASIC CNN WITH CROSS VALIDATION

This approach is useful for improving simulation model efficiency. It demonstrates how a neural network can perform on a separate data set. Serial correlation is critical for the future of a model's assumptions in studies and education. The dataset into two parts by different classifiers.. The first is for preparation, and the second is for screening or validation. Cross testing is a method for template matching on a test dataset and then testing its results vs a test dataset. Furthermore, during the learning process, serial correlation checks the prototype to see if there is some over and to get an understanding as to how the system will behave on unrelated results. Besides that, when multiple verifications are conducted, serial correlation requirement changes. To determine the validity, the outcomes from all of the bounces are summed. In a nutshell, purposeful sampling is used to report the accuracy of new approaches on the very same sample.. Test dataset is often used to find the best variables for a template. Figure 4.2 depicts our simple Cnn architecture, as well as an exemplar of algorithm division for testing data.

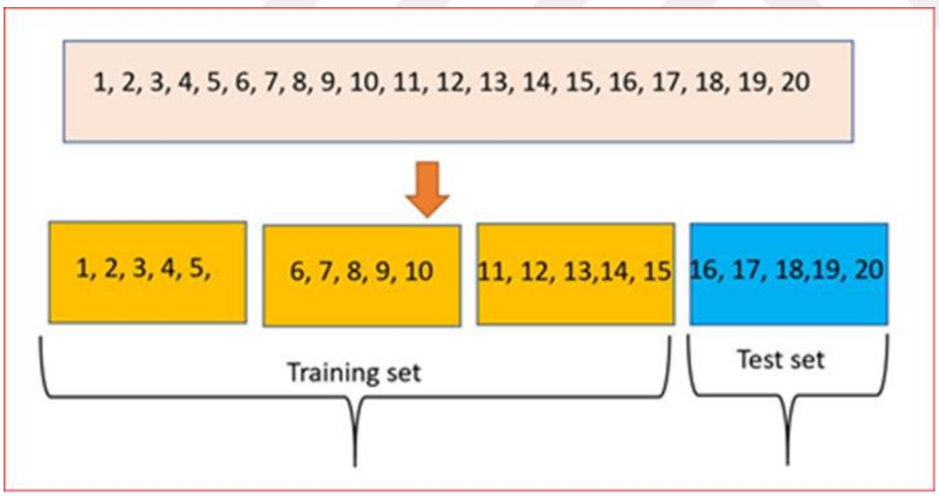


**Figure 4.2:** An example of Dividing Dataset for Cross Validation

## 4.2 K-FOLD

The most popular test dataset method in computer vision is K-fold. The source program is split into k equivalent subsets by K fold. Each one is referred to as a fold. Then it maintains one fold as a verification and uses the remaining k-1 folds for preparation. After the project is done then it checks the ability of the prediction by justifying the expected result against that folds held for verification. The entire process will be repeated test dataset more with a structural elucidation package. This implies that each entry is only validated once. The method computes the precision by combining the observations since all of them would have been measured and compiled. Since the majority of information is being used for both fit and verification, out and under-fitting of the template can be treated.

Figure 4.3. shows the k-fold mechanism for the value of k=10.

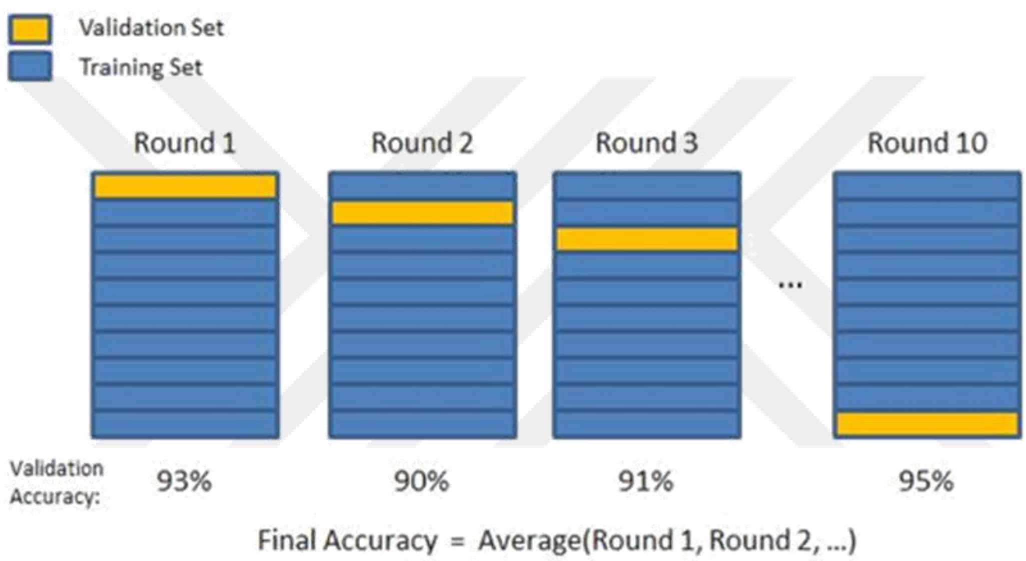


**Figure 4.3:** K-Fold Mechanism

### 4.3 APPLYING CNN WITH CROSS-VALIDATION

We used CNN with just Relu activation function, two at the very most layers, and two drop - outs layers with one of the at the start of the testing period. To begin the process, all you need is a simple CNN. After that, we used 1 soften sheet. And we used this to train our model. We illustrated how our template reacts to our database after we conditioned it with this basic CNN.. After that, we modified our model using the cross-validation method. To test the concept, we divided our datasets into three parts. So, then what will occur is that the prior Convolution layer will be tested anew, however this period with a small but successful change. Since we divided our datasets into three folds, the CNN should take multiple ways, one as a classification algorithm and the other two as classification model. The very first splitting will be the validity set, and the second three splits will be the pretreatment during the first phase. The second break will be used for verification, while the first and third splits will be used for preparation. The test data would be the last break at the top, although the first two will be the normal distribution. The reliability would suffer as a result of breaking the very same database several years with water greater stability. Afterward, we'll check the result of numerous CNN architectures on our set of data and selecting the optimal framework for completing work on it.

The template we developed to conduct CNN on our datasets is shown in Figure 4.4.

```
Model: "sequential_2"
_________________________________________________________________
Layer (type)                 Output Shape              Param #
=================================================================
conv2d_3 (Conv2D)            (None, 224, 224, 64)      1792
_________________________________________________________________
max_pooling2d_3 (MaxPooling2 (None, 112, 112, 64)      0
_________________________________________________________________
dropout_3 (Dropout)          (None, 112, 112, 64)      0
_________________________________________________________________
conv2d_4 (Conv2D)            (None, 112, 112, 64)      36928
_________________________________________________________________
max_pooling2d_4 (MaxPooling2 (None, 56, 56, 64)        0
_________________________________________________________________
dropout_4 (Dropout)          (None, 56, 56, 64)        0
_________________________________________________________________
flatten_2 (Flatten)          (None, 200704)            0
_________________________________________________________________
dense_3 (Dense)              (None, 128)               25690240
_________________________________________________________________
dense_4 (Dense)              (None, 2)                 258
=================================================================
Total params: 25,729,218
Trainable params: 25,729,218
Non-trainable params: 0
```

**Figure 4.4:** Build Architecture of CNN model

Our model's loss, reliability, non - existent, and test dataset per 5 epochs are shown in the table below. It can be seen that the reliability was improving across period while the error was decreasing.

**Table 4.1:** Outputs per 5 epochs in CNN Architecture

| Number Of Epochs | Loss | Accuracy | Val Loss | Val Accuracy |
|---|---|---|---|---|
| 5 | 0.8950 | 0.5946 | 0.5840 | 0.7481 |
| 10 | 0.6985 | 0.6458 | 0.5388 | 0.7443 |
| 15 | 0.6251 | 0.6757 | 0.5464 | 0.6780 |
| 20 | 0.5924 | 0.6970 | 0.5513 | 0.6780 |
| 25 | 0.5920 | 0.6927 | 0.5504 | 0.6856 |
| 30 | 0.5947 | 0.6861 | 0.5540 | 0.6686 |
| 35 | 0.5857 | 0.6927 | 0.5545 | 0.6648 |
| 40 | 0.5889 | 0.6965 | 0.5533 | 0.6667 |
| 45 | 0.5798 | 0.7032 | 0.5530 | 0.6705 |
| 50 | 0.5848 | 0.6918 | 0.5535 | 0.6686 |

We obtained by plotting the validity and deterioration of each era before creating the accuracy of the model to visualise the teaching ow of our framework. A json file was developed. We also saved the model's weight in an HDF5 le file so that we could use it in future studies. These tasks were completed for each design we used on the database.. The reliability and failure of our template during the learning phase are visualized in Fig 4.5.

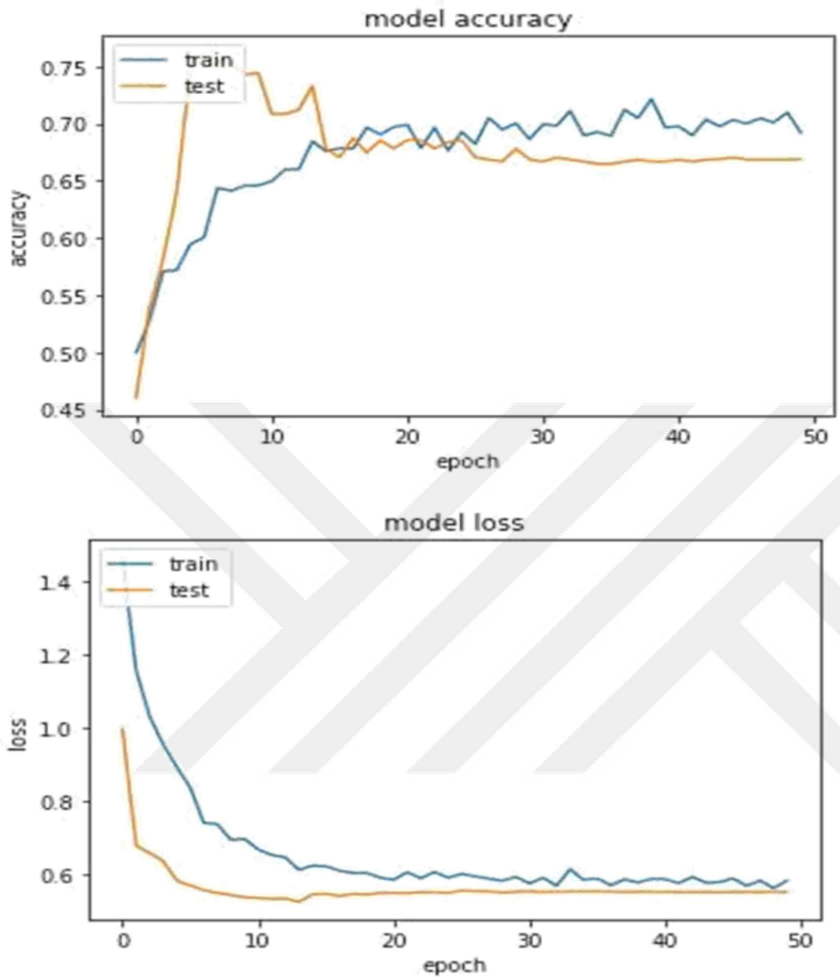


**Figure 4.5:** Loss Vs epochs.

Deep Cnn Reliability (precision vs. iterations) and System Failure (**Figure 4.5**). (loss vs epochs)

Figure 4.6VGG16's design is depicted in.

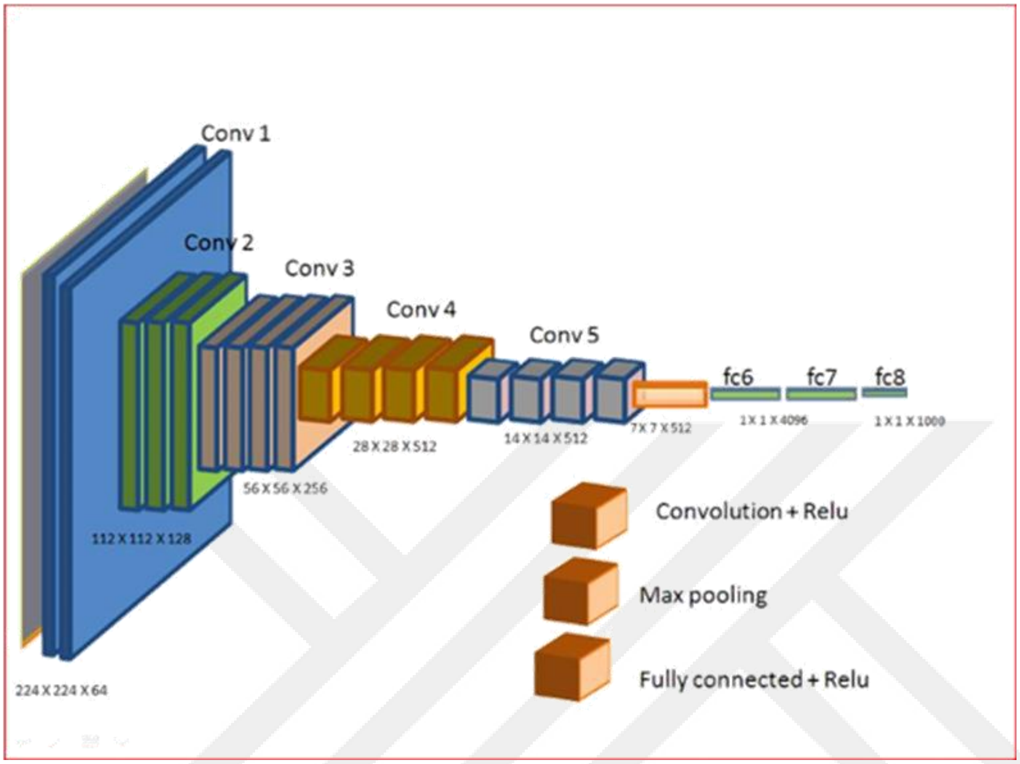


**Figure 4.6:** VGG16

## 4.4 APPLYING VGG16 IN OUR DATASET

To confirm the adequacy of our sample, we used VGG16 design to practice our template. We fed the template the very same criteria and started teaching it. Our set of data yielded 91.303 percent share after teaching our method with VGG16.

**Table 4.2:** Outputs per 5 epochs in VGG16 Architecture.

| Number of Epochs | Loss | Accuracy | Val Loss | Val Accuracy |
|---|---|---|---|---|
| 5 | 0.4910 | 0.7534 | 0.5031 | 0.7595 |
| 10 | 0.4502 | 0.7790 | 0.4211 | 0.8030 |
| 15 | 0.3783 | 0.8236 | 0.3910 | 0.8106 |
| 20 | 0.3624 | 0.8359 | 0.3760 | 0.8163 |
| 25 | 0.3270 | 0.8440 | 0.3528 | 0.8447 |
| 30 | 0.3011 | 0.8615 | 0.3835 | 0.8239 |
| 35 | 0.2812 | 0.8677 | 0.3628 | 0.8447 |
| 40 | 0.2552 | 0.8810 | 0.3699 | 0.8390 |
| 45 | 0.2388 | 0.8928 | 0.3660 | 0.8466 |
| 50 | 0.2321 | 0.8976 | 0.3637 | 0.8523 |

Figure 4.7 shows the accuracy and loss of VGG16 throughout the training process.

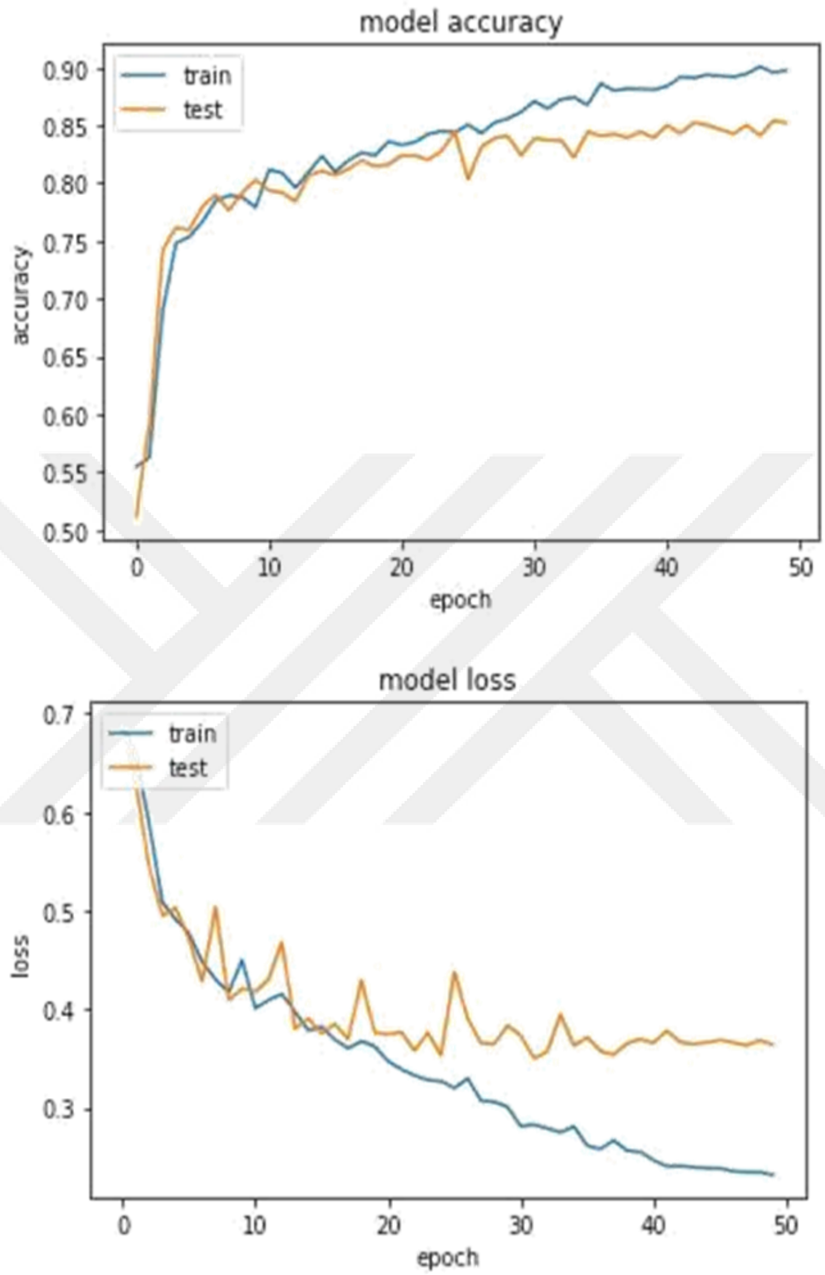


**Figure 4.7:** VGG16 Model Accuracy (accuracy vs epochs) and Model Loss (loss vs epochs)

### 4.5 VGG19

The only distinction between VGG19 and VGG16 is that VGG19 has 3 main levels with very narrow (33) convolutional layers. VGG19's design is depicted in Figure 4.8.

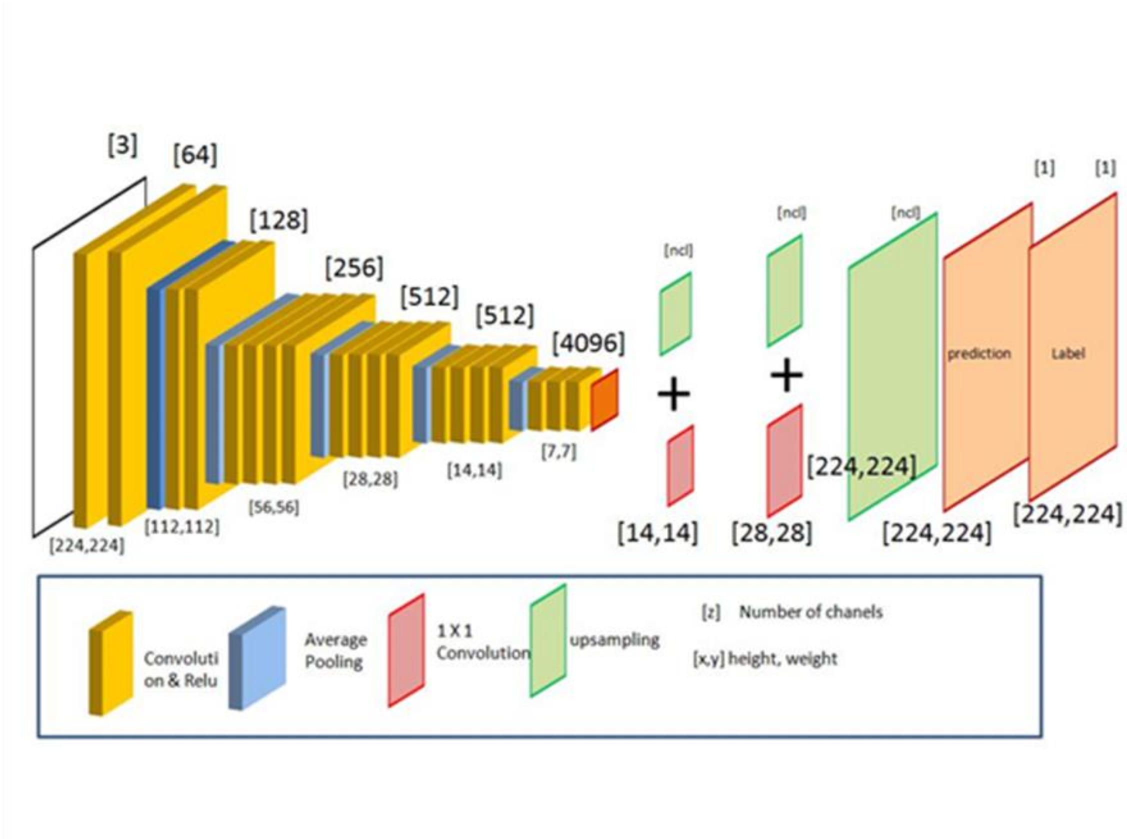


**Figure 4.8:** VGG19

#### 4.5.1 Applying VGG19 in Our Dataset

We used the VGG19 framework to practice our template that used the same variables to calculate the precision of our datasets. Our database obtained an accuracy of 84.545 percent after practicing our template with VGG19. The table 2 show the failure, error, and non - existent and precision for VGG19 over 5 eras.

**Table 4.3:** Outputs per 5 epochs in VGG19 Architecture

| Number of Epochs | Loss | Accuracy | Val Loss | Val Accuracy |
|---|---|---|---|---|
| 5 | 0.5042 | 0.7549 | 0.6090 | 0.6932 |
| 10 | 0.4403 | 0.7876 | 0.4094 | 0.8030 |
| 15 | 0.3890 | 0.8004 | 0.3868 | 0.8068 |
| 20 | 0.3594 | 0.8255 | 0.3983 | 0.8087 |
| 25 | 0.3311 | 0.8421 | 0.4045 | 0.8239 |
| 30 | 0.3182 | 0.8464 | 0.3724 | 0.8352 |
| 35 | 0.2696 | 0.8725 | 0.3789 | 0.8409 |
| 40 | 0.2628 | 0.8796 | 0.3941 | 0.8277 |
| 45 | 0.2227 | 0.8971 | 0.4001 | 0.8277 |
| 50 | 0.2009 | 0.9161 | 0.3781 | 0.8447 |

Figure 4.9 shows accuracy and loss of VGG19 throughout the training process.

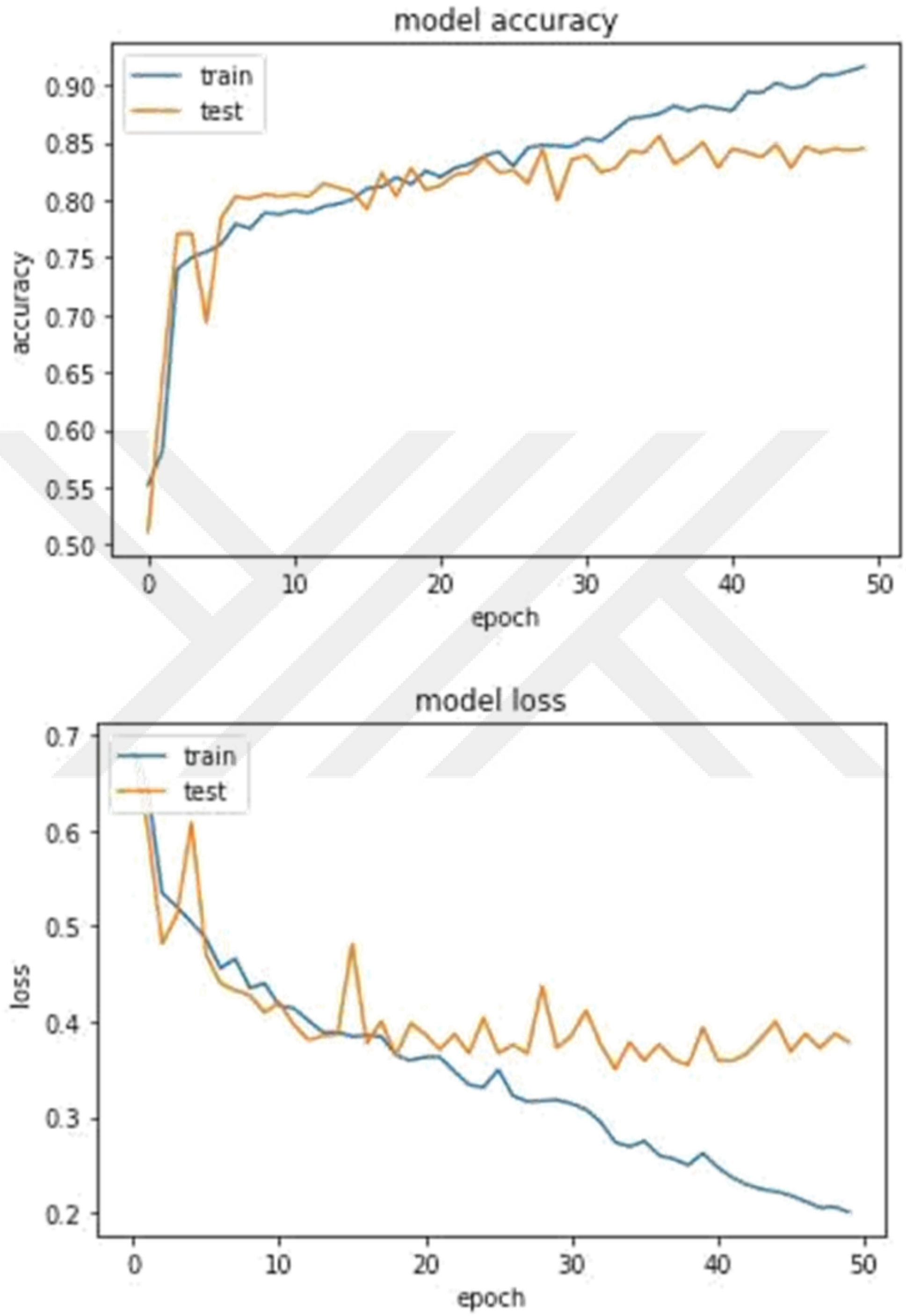


**Figure 4.9:** VGG19 Model Accuracy (accuracy vs epochs) Model Loss(loss vs epochs)

## 4.6 XCEPTION COCEPT

Severe variant of Conception with feature extraction matrices is referred to as Series of intervals. The site nxn dimensional regularization is referred to as convolution layer. There will be 5 nxn temporal linear combination if a surface has three streams. Xception is valued higher than Convolution layer on two architectures. Initial feature extraction activation function and modified feature maps linear interpolation are the two forms of feature extraction matrix multiplication. The pooling layers normalization is accompanied by a point - wise matrix multiplication in the initial depth - wise separable conversation. The 1x1 regularization to alter the aspect is called point - wise clustering. Regularization is not performed through all sources in feature extraction matrix multiplication, as it is in traditional matrix multiplication. As a result, this is a practical solution because the model is optimized, the template is more accurate, and the system is light. Changed depth wise activation function, but at the other hand, is cost function concatenation accompanied by convolutional layers. This modification is based on Iteration v3's 1x1 matrices while conducting nxn contextual regularization. Furthermore, SVM has been the most effective method for displaying the average precision estimation when two atoms occur in a digital object.

The initial pooling layer regularization in Social media has turned is shown in Figure 4.9.

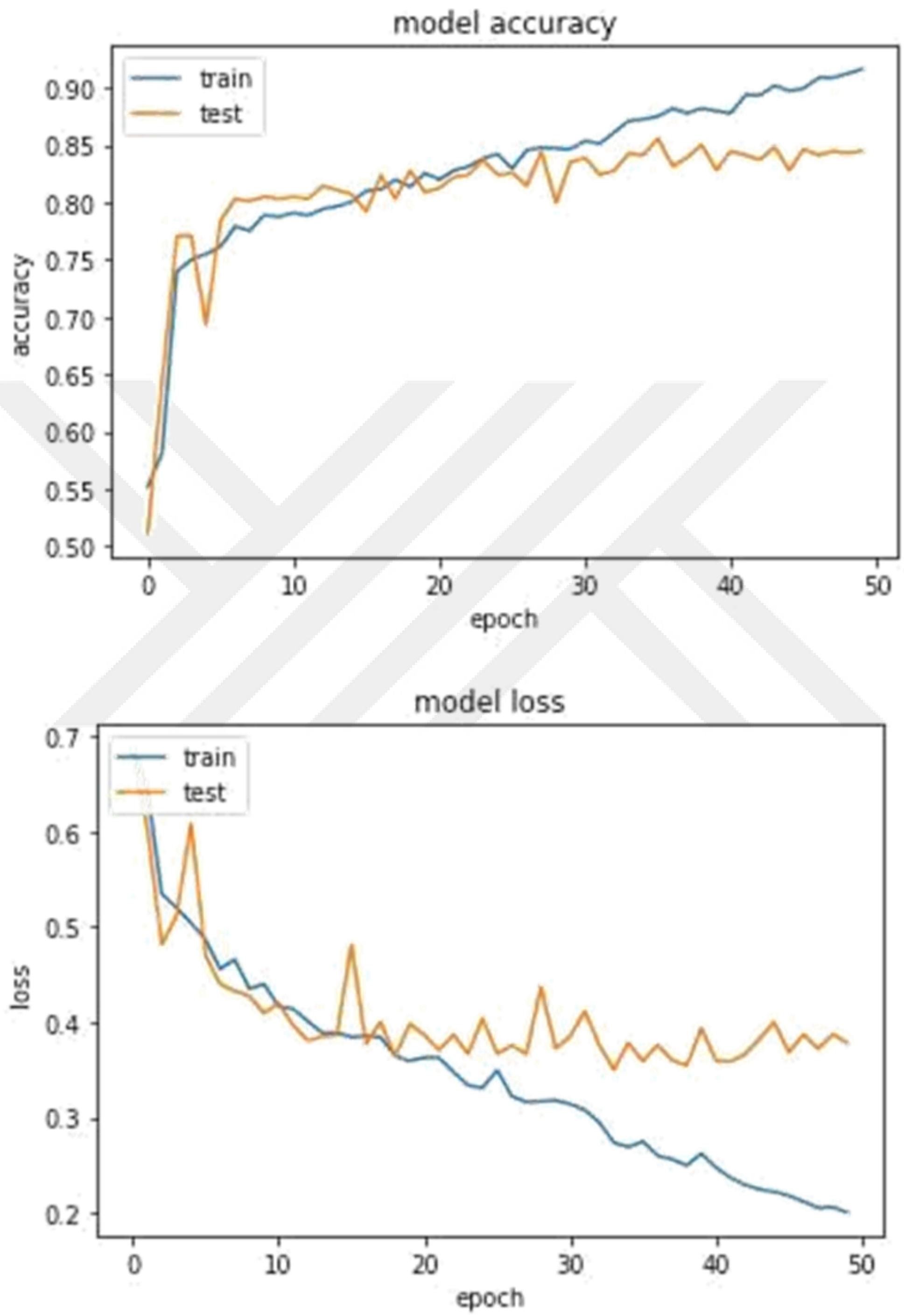


**Figure 4.10:** Original Xception

Figure 4.10 shows the modified depth wise separable convolution in xception.

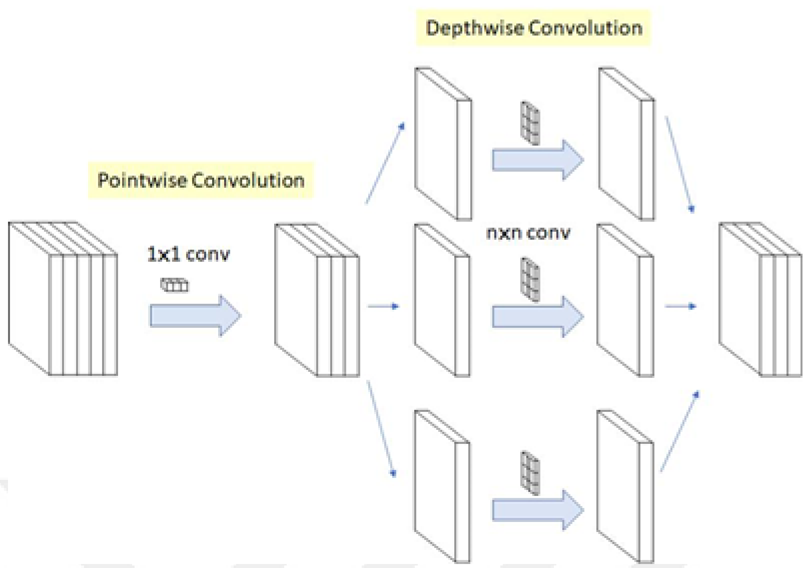


**Figure 4.11:** Modified Xeption

### 4.6.1 Applying Xception in Our Dataset

We used Hopfield technology to practice the template after implementing VGG19 to determine the validity of our datasets. We followed the same procedure as they did for other frameworks, maintaining all other variables at their default values. After testing our template with Series of intervals, we got around 85.303 percent precision from our datasets.

The table 2 show the Hopfield error, error, validity deterioration, and test dataset over five eras. It can be seen that the reliability was improving over time while the error was decreasing.

**Table 4.4:** Outputs per 5 epochs in Xception Architecture

| Number of Epochs | Loss | Accuracy | Val Loss | Val Accuracy |
|---|---|---|---|---|
| 5 | 0.3301 | 0.8492 | 0.6911 | 0.5360 |
| 10 | 0.2418 | 0.9047 | 0.6942 | 0.5360 |
| 15 | 0.1891 | 0.9350 | 0.7985 | 0.5360 |
| 20 | 0.1702 | 0.9426 | 0.9698 | 0.5379 |
| 25 | 0.1384 | 0.9606 | 0.4709 | 0.7803 |
| 30 | 0.1246 | 0.9625 | 0.3569 | 0.8220 |
| 35 | 0.1020 | 0.9768 | 0.3543 | 0.8295 |
| 40 | 0.0809 | 0.9829 | 0.3598 | 0.8371 |
| 45 | 0.0747 | 0.9853 | 0.3662 | 0.8295 |
| 50 | 0.0678 | 0.9867 | 0.3709 | 0.8314 |

Figure 4.12 shows the accuracy and loss of Xception throughout the training process.

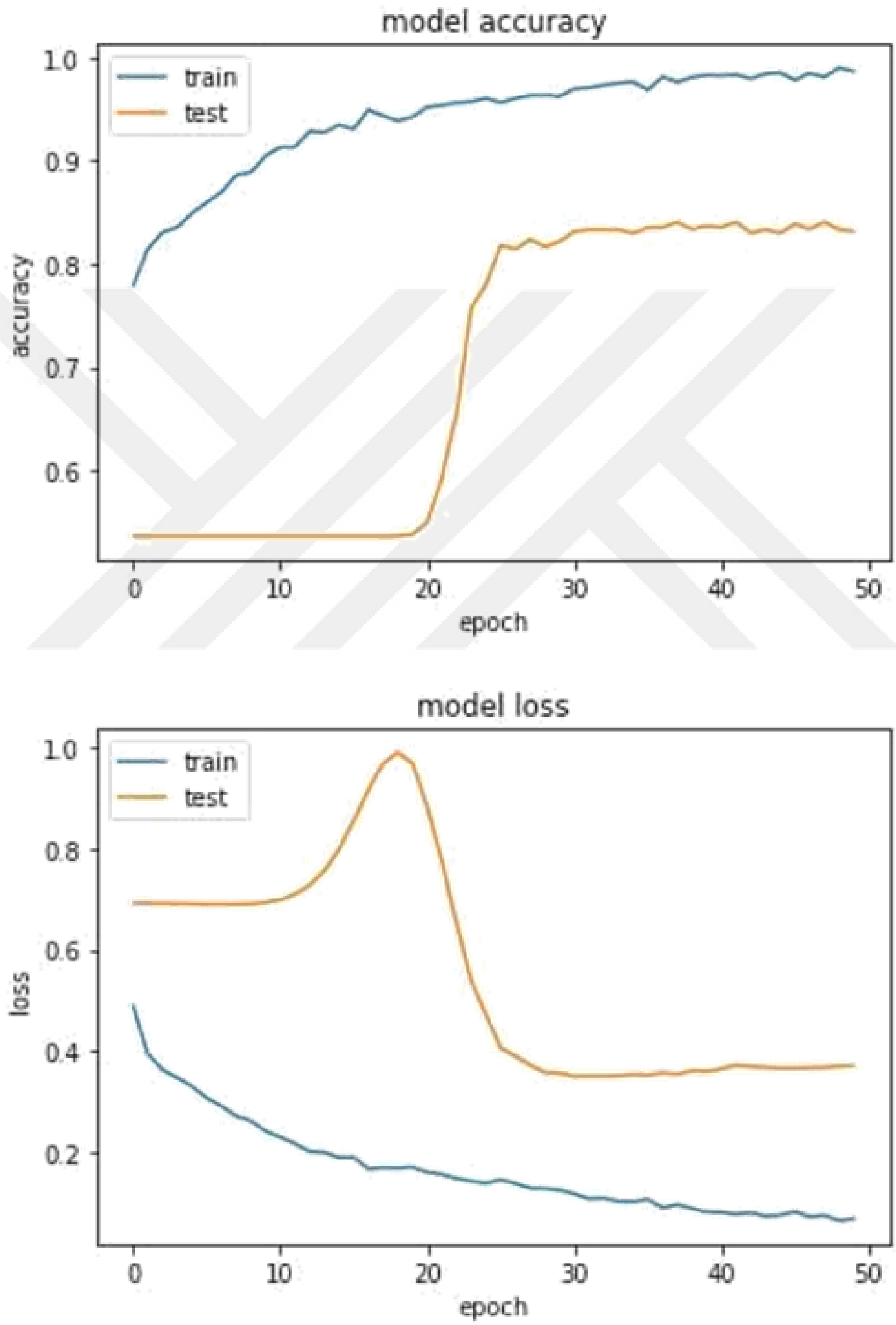


**Figure 4.12:** Xception Model Accuracy(accuracy vs epochs) Model Loss(loss vs epochs)

Figure 4.13 shows 10 sample images from the dataset along with their labels.

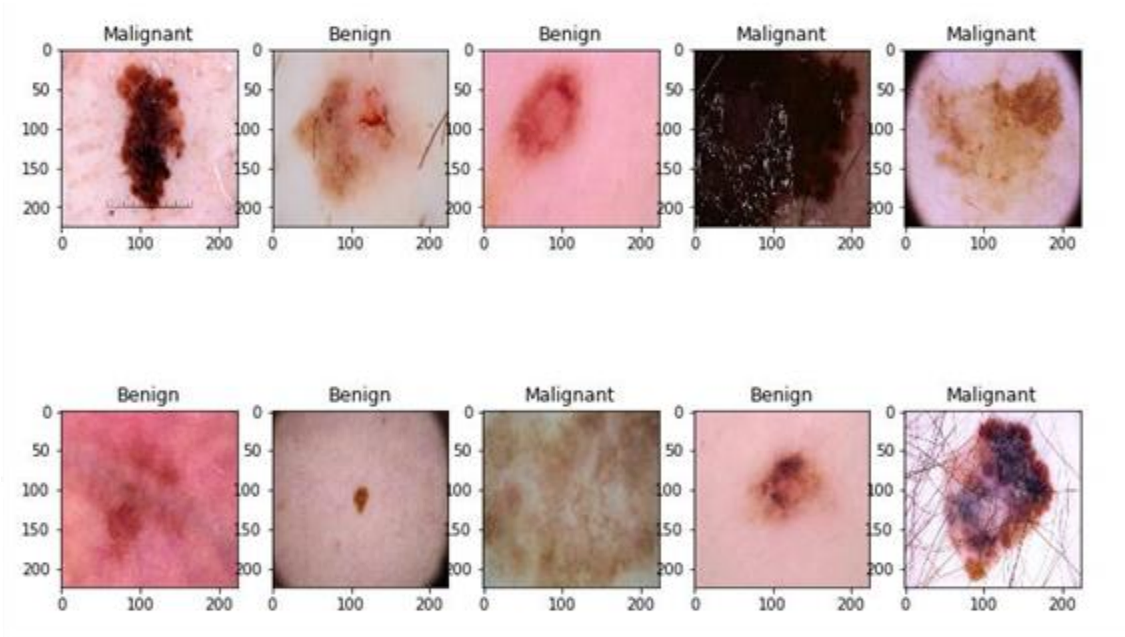


**Figure 4.13:** Output of original test data

Figure 4.14 shows the prediction of Xception on those images

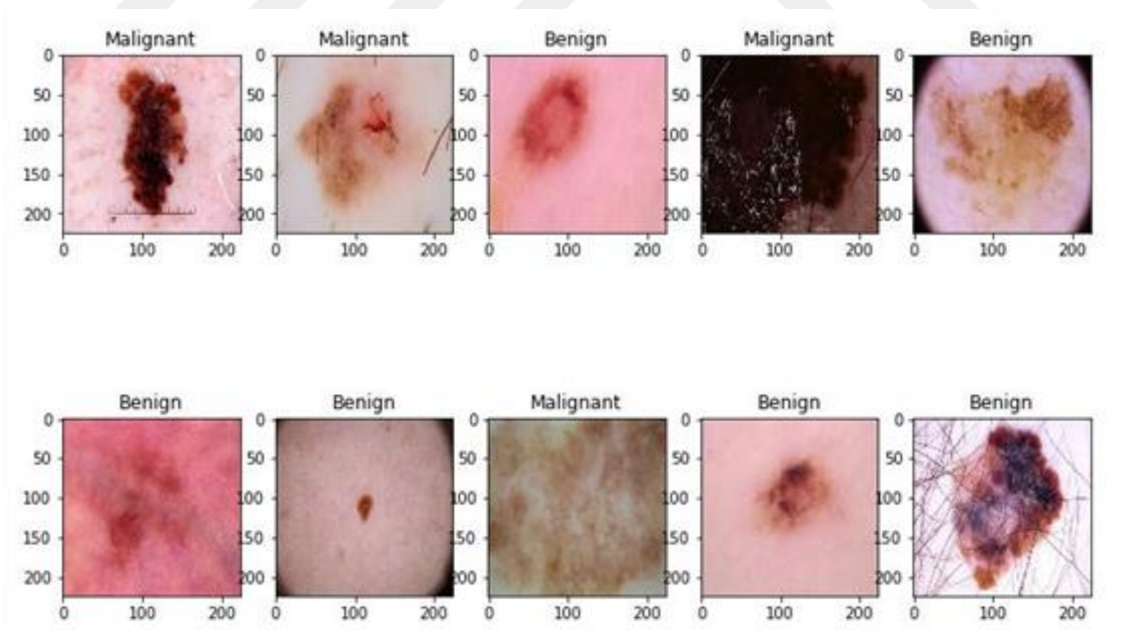


**Figure 4.14:** Xception prediction on the same test data

# 5. DISCUSSION

Skin infection is the most common clinical problem that affects a large number of people around the globe. The development of dermatological perceptive organization is becoming progressively perceptive and accurate as a result of the rapid development of inventions and the use of various knowledge extraction techniques as of lately.. As a result, it's important to develop AI techniques that can properly distinguish skin nausea orders. Until now, no technique has beaten all the others when it comes to applying AI to skin condition prediction. Strategies: In a previous research paper [39], a technique was presented, in which five different data mining techniques were used to create a community solution that included all five different picture handling approaches as a single system. We examine various picture handling protocols to classify the skin ailment and aft using informative Neurosurgery data., An artificial intelligence (AI) methodology is used to create the outfit. Tends to result: The local plan method, which is based on AI, was tested on Neurosurgery databases and was able to classify skin diseases into six distinct groups, including C1: rosacea, C2: alopecia psoriasis, C3: fungus find many examples, C4: candidiasis dendrobiums, C5: persistent inflammation, and C6: candidiasis rotala.. The results show that when compared to a single classification model, the urological prediction accuracy of the test informative set is increased. End: As compared to other classification model estimates, the collecting approach used on Neurosurgery databases looks nicer. The use of a collecting technique allows for a more accurate and effective skin illness prediction. In the healthcare profession, severe bacterial diseases are one of the most popular signs of diseases. It is commonly identified externally, beginning with a physical exam and probably accompanied by dermoscopy images review, medicines either systemic and injectable, and histological review. In this study I will concentrate on classifiers like CNN and Data Collected Identification for Detecting Vaginal Skin Disease [40]. Machine learning is constantly being used to improve the precision of identifying various clinical conditions. Many new methods have been developed to speed up the process while maintaining the highest standards of precision. In this study, we presented a framework for even more like have infectious diseases by combining computer vision with artificial neural networks, a form of computer vision phenomenon found in computer vision.

# 6. CONCLUSION

The aim of this study is to find and propose a proper Cnn architecture that can be educated and used to more level factors surface infectious diseases. While our study, we discovered a few thesis works in this area. Even so, the majority of the reporting was done exclusively for CNN. We came up with the concept of contrasting Neural networks, and we got a very good test out of everything. We used other experimental studies to help us train our system with CNN, and we had to test our objects with two Classification algorithms on our own.. We might improve our template by changing the size, such as expanding the amount of eras, decreasing the scale factor, adjusting the price of slacker, and so on, but this will naturally take much longer. For our database, the compared to the leading we find gave out nearly 91.303 percent share.. Because of the small energy machine and other variables such as database dynamic range and picture before the, there is a risk of having reduced precision. An issue that could arise is the fact that CNN takes a long time to digest and educate digital images. Furthermore, we had a database with identical kinds of pictures, because when we tested it for network deployment, the reliability could be lower than what we've had.

### Future Work

Using CNN and its frameworks to identify microbial skin problems has a lot of room for improvement. The world is evolving at a breakneck pace, and engineering, together with the entire computing world, is following suit. All is becoming more powerful and quicker.. As a result, with a stronger object classification algorithm, we could be able to increase our prediction performance and prescribe medication in finding skin infectious diseases sooner. Keras also allows users to design and develop their own CNN models based on their specific requirements. Thus, by studying all of the implications of all of the variables used in our design, we will build our specific Cnn that will solve all of the barriers to more detect known surface infectious diseases.. Furthermore, we are still attempting to determine the best method for combining all of the frameworks and then displaying the total score, a practice called as clustering. We're operating on two forms of assembly: the first is averaging the results obtained within each design and then predicting the performance of a test dataset with one of the most expected values from both designs.. The second is to train each method in turn, using the expected performance from the original version as the feedback during the next version, and then to complete all of the formulas in the system. A further essential issue we are attempting to complete as part of our research is to incorporate our database into CSV files, transform mechanism into quantitative data, and use neural networks to enhance the precision of our developed framework.

# REFERENCES


[1] S. Jain, N. Pise, et al., \Computer aided melanoma skin disease detection using image processing", Procedia Computer Science, vol. 48, pp. 735-740, 2015.

[2] Simonyan, Karen, Zisserman, and Andrew, Very deep convolutional networks for large-scale image recognition, Apr. 2015. [Online]. Available: https://arxiv. org/abs/1409.1556/.

[3] M. H. Jafari, N. Karimi, E. Nasr-Esfahani, S. Samavi, S. M. R. Soroushmehr, K. Ward, and K. Najarian, \Skin lesion segmentation in clinical images using deep learning", in 2016 23rd International conference on pattern recognition (ICPR), IEEE, 2016, pp. 337-342.

[4] J. Kawahara, A. BenTaieb, and G. Hamarneh, \Deep features to classify skin lesions", in 2016 IEEE 13th International Symposium on Biomedical Imaging (ISBI), IEEE, 2016, pp. 1397-1400.

[5] E. Nasr-Esfahani, S. Samavi, N. Karimi, S. M. R. Soroushmehr, M. H. Jafari, K. Ward, and K. Najarian, \Melanoma detection by analysis of clinical images using convolutional neural network", in 2016 38th Annual International Conference of the IEEE Engineering in Medicine and Biology Society (EMBC), IEEE, 2016, pp. 1373-1376.

[6] V. Pomponiu, H. Nejati, and N.-M. Cheung, \Deepmole: Deep neural networks for Bacterial Skin Infection ", in 2016 IEEE International Conference on Image Processing (ICIP), IEEE, 2016, pp. 2623{2627.

[7] A. Esteva, B. Kuprel, R. A. Novoa, J. Ko, S. M. Swetter, H. M. Blau, and S.Thrun, Dermatologist-level classi cation of skin diseases with deep neural networks, Jan. 2017. [Online]. Available: https://www.nature.com/articles/ nature21056? draft=collection&proof=true.

[8] S. Hershey, S. Chaudhuri, D. P. Ellis, J. F. Gemmeke, A. Jansen, R. C. Moore, M. Plakal, D. Platt, R. A. Saurous, B. Seybold, et al., \CNN architectures for large-scale audio classification", in 2017 IEEE international conference on acoustics, speech and signal processing (icassp), IEEE, 2017, pp. 131-135.

[9] M. Hollemans, Compressing deep neural nets, Sep. 2017. [Online]. Available: https://machinethink.net/blog/compressing-deep-neural-nets/.

[10] Convolutional neural network (CNN), Oct. 2018. [Online]. Available: https:// developer.nvidia.com/discover/convolutional-neural-network.

[11] Verma, Anurag & Pal, Saurabh & Kumar, Surjeet. (2019). Classification of Skin Disease using Ensemble Data Mining Techniques. Asian Pacific journal of cancer prevention: APJCP. 20. 1887-1894. 10.31557/APJCP.2019.20.6.1887.

[12] Alazab, A.; Abawajy, J.; Hobbs, M.; Layton, R.; Khraisat, A. Crime toolkits: the productisation of cybercrime. In Proceedings of the 2013 12th IEEE International Conference on Trust, Security and Privacy in Computing and Communications, Melbourne, Australia, 16–18 July 2013; pp. 1626–1632.

[13] Available Online: https://www.researchgate.net/figure/Architecture-of-a-Convolutional-Neural-Network-CNN-The-traditional-CNN-structure-is_fig1_330106889

[14] Available Online:https://www.i2tutorials.com/hidden-layers-in-neural-networks/

[15] Available Online: https://stackabuse.com/deep-learning-in-keras-building-a-deep-learning-model/

[16] Available Online: https://www.researchgate.net/figure/Outline-of-the-convolutional-layer_fig1_323792694

[17] Available Online: https://link.springer.com/article/10.1186/s13321-020-00436-5

[18] Available Online: https://www.geeksforgeeks.org/cnn-introduction-to-pooling-layer/

[19] Available Online: https://www.quora.com/What-are-the-main-normalization-layers-in-artificial-neural-networks

[20] Available Online: https://www.arxiv-vanity.com/papers/1712.01252/

[21] Available Online:https://towardsdatascience.com/everything-you-need-to-know-about-neural-networks-and-backpropagation-machine-learning-made-easy-e5285bc2be3a

[22] Available Online:https://textimgs.s3.amazonaws.com/boundless-psychology/1206-the-neuron.jpe

[23] Committee on Diagnostic Error in Health Care, Board on Health Care Services, Institute of Medicine, The National Academies of Sciences, Engineering and Medicine, Improving Diagnosis in Health Care.National Academies Press (US), 2015.

[24] N.V.K. Medathati, H. Neumann, G.S. Masson, P. Kornprobst, “Bio-inspired computer vision: Towards a synergistic approach of artificial and biological vision,” Computer Vision and Image Understanding, April 2016.

[25] K. Fukushima, “Artificial vision by multi-layered neural networks: neocognitron and its advances,”Neural Networks, vol. 37, pp. 103–119, 2013.

[26] Available Online: https://www.jeremyjordan.me/content/images/2018/03/Screen-Shot-2018-03-06-at-3.17.13-PM.png

[27]https://www.researchgate.net/publication/318204554/figure/fig1/AS:512595149770752@1499223615487/Autoencoder-architecture.png

[28] https://www.mdpi.com/applsci/applsci-10-02488/article_deploy/html/images/applsci-10-02488-g003.png

[29] Cho, E.J.; Kim, J.H.; Hong, C.S. Attack Model and Detection Scheme for Botnet on 6LoWPAN; Springer: Berlin/Heidelberg, Germany, 2009; pp. 515–518.

[30] Moustafa, N.; Turnbull, B.; Choo, K.R. An Ensemble Intrusion Detection Technique based on proposed Statistical Flow Features for Protecting Network Traffic of Internet of Things. IEEE Internet Things J. 2019, 6, 4815–4830. [CrossRef]

[31] Cervantes, C.; Poplade, D.; Nogueira, M.; Santos, A. Detection of sinkhole attacks for supporting secure routing on 6LoWPAN for Internet of Things. In Proceedings of the 2015 IFIP/IEEE International Symposium on Integrated Network Management (IM), Ottawa, ON, Canada, 11–15 May 2015; pp. 606–611.

[32] Venkatraman, S.; Surendiran, B. Adaptive hybrid intrusion detection system for crowd sourced multimedia internet of things systems. Multimed. Tools Appl. 2019, 1–8. [CrossRef]

[33] Patil, R.; Modi, C. Designing a Virtual Environment Monitoring System to Prevent Intrusions in Future Internet of Things; Springer: Singapore, 2019; pp. 345–351.

[34] Kenkre, P.S.; Pai, A.; Colaco, L. Real Time Intrusion Detection and Prevention System. In Proceedings of the 3rd International Conference on Frontiers of Intelligent Computing: Theory and Applications (FICTA) 2014, Bhubaneswar, India, 14–15 November 2014; Satapathy, S.C., Biswal, B.N., Udgata, S.K., Mandal, J.K., Eds.; Springer International Publishing: Cham, Switzerland, 2015; Volume 1, pp. 405–411.

[35] Liao, H.J.; Lin, C.H.R.; Lin, Y.C.; Tung, K.Y. Intrusion detection system: A comprehensive review. J. Netw. Comput. Appl. 2013, 36, 16–24. [CrossRef]

[36] Ashfaq, R.A.R.; Wang, X.Z.; Huang, J.Z.; Abbas, H.; He, Y.L. Fuzziness based semi-supervised learning approach for intrusion detection system. Inf. Sci. 2017, 378, 484–497.

[37] Al-Yaseen, W.L.; Othman, Z.A.; Nazri, M.Z.A. Multi-level hybrid support vector machine and extreme learning machine based on modified K-means for intrusion detection system. Expert Syst. Appl. 2017, 67, 296–303.

[38] Alazab, A.; Hobbs, M.; Abawajy, J.; Alazab, M. Using feature selection for intrusion detection system. In Proceedings of the 2012 International Symposium on Communications and Information Technologies (ISCIT), Gold Coast, Australia, 2–5 October 2012; pp. 296–301.

[39] Gray, R.M. Entropy and Information Theory; Springer: Berlin/Heidelberg, Germany, 2017.

[40] Khraisat, A.; Gondal, I.; Vamplew, P. An Anomaly Intrusion Detection System Using C5 Decision Tree Classifier. In Trends and Applications in Knowledge Discovery and Data Mining; Springer International Publishing: Cham, Switzerland, 2018; pp. 149–155.